

A Review of Aeronautical Fatigue Investigations in Brazil

International Committee on Aeronautical Fatigue and Structural Integrity (ICAF)

Nagoya – Japan – June 2017



Prepared by:

Carlos E. Chaves

On behalf of:

Fatigue, Fracture and Structural Integrity Committee

Brazilian Society of Engineering and Mechanical Sciences - ABCM



ICAF2017
35th Conference
29th Symposium
Nagoya, JAPAN
© ICAF2017 Organizing Committee

A Review of Aeronautical Fatigue Investigations in Brazil ICAF 2017 – Nagoya - Japan



SUMMARY

This report presents the review of fatigue investigations related to aeronautics performed in Brazil during the years 2015 to 2017. Its contents will be presented during the 35th ICAF (International Committee on Aeronautical Fatigue and Structural Integrity) Conference to be held in Nagoya, Japan, in June 05, 2017.

Some of the works were previously presented in other conferences or are available from public sources. All other papers were directly supplied by their authors to the author of this review.

COVER: E190-E2 Full-scale Fatigue Test Article - Initial Preparations.



CONTENTS

1. INTRODUCTION	8
2. ANALYSIS AND SIMULATION	9
3. METALLIC MATERIALS – FATIGUE AND FRACTURE PROPERTIES	12
4. METALLIC MATERIALS – PROCESSES	13
5. METALLIC MATERIALS – STRUCTURES	17
6. COMPOSITE MATERIALS	25
7. COMPOSITE MATERIALS – STRUCTURES	33
8. HYBRID STRUCTURES	34
9. STRUCTURAL HEALTH MONITORING	38
10. FATIGUE LIFE MONITORING	42
11. MISCELLANEOUS	44
12. REFERENCES	45

ABBREVIATIONS

ABCM	Associação Brasileira de Engenharia e Ciências Mecânicas (Brazilian Society of Engineering and Mechanical Sciences)
ANAC	Agência Nacional de Aviação Civil (Brazilian Aviation Agency)
ASTM	American Society for Testing and Materials
CAI	Compression After Impact
CCS	Compact Compressive Specimen
CFRP	Carbon Fiber Reinforced Polymer
CF-PPS	Carbon Fiber-reinforced Poly (Phenylene Sulfide)
CLS	Cracked Lap Shear (Specimen)
COBEM	Congresso Internacional de Engenharia Mecânica (International Congress of Mechanical Engineering)
DCTA	Departamento de Ciência e Tecnologia Aeroespacial (Department of Aerospace Science and Technology)
CVM	Comparative Vacuum Monitoring
DCB	Double Cantilever Beam
DCT	Displacement Correction Technique
DEN	Double Edge Notched (Specimen)
EMB	Embraer
ERJ	Embraer Regional Jet
FAB	Força Aérea Brasileira (Brazilian Air Force)
FCG	Fatigue Crack Growth
FDG	Fatigue Disbond Growth
FEM	Finite Element Method
FML	Fiber Metal Laminate
FSFT	Full-Scale Fatigue Test
FSW	Friction Stir Welding
GA	Genetic Algorithm
GFEM	Global Finite Element Method
HLUP	Hand Lay-Up
HZG	Helmholtz-Zentrum Geesthacht

IPT	Instituto de Pesquisas Tecnológicas (Institute for Technological Research)
ITA	Instituto Tecnológico de Aeronáutica (Aeronautical Institute of Technology)
ISQ	Instituto de Soldadura e Qualidade
LVI	Low Velocity Impact
LW	Lamb Waves
MMB	Mixed-Mode Bending
MSD	Multi-Site Damage
OEM	Original Equipment Manufacturer
POD	Probability of Detection
R&D	Research and Development
RRA	Retrogression and Re-Ageing
TRL	Technology Readiness Level
S/A	Sociedade Anônima (Corporation)
SERR	Strain Energy Release Rate
SENB	Single Edge Notched (Specimen) in Bending
SG	Strain Gage
SHM	Structural Health Monitoring
SLJ	Single Lap Joint
SP	São Paulo (State)
SSAI	Shear Strength After Impact
S-SHM	Scheduled Structural Health Monitoring
SwRI	Southwest Research Institute
TUHH	Hamburg University of Technology
UEPG	Universidade Estadual de Ponta Grossa (State University of Ponta Grossa)
UFMG	Universidade Federal de Minas Gerais (Federal University of Minas Gerais)
UFSCar	Universidade Federal de São Carlos (Federal University of São Carlos)
UNICAMP	Universidade de Campinas (University of Campinas)
UNIFEI	Universidade Federal de Itajubá (Federal University of Itajubá)
UNESP	Universidade Estadual Paulista (State University of São Paulo)
USP	Universidade de São Paulo (University of São Paulo)
VaRTM	Vacuum Assisted Resin Transfer Molding

INDEX OF FIGURES

Figure 1 – Splitting Method - Numerical Example.	11
Figure 2 – Example of application – three cracks on the edge of holes.	11
Figure 3 – Selected results from Ref. [6]. (a) geometry of the compact tension Al alloy specimen (dimensions in mm), (b) fatigue crack growth rate versus ΔK curves for the three aged conditions, (c) COD in the function stress intensity factor, ΔK , from the T7451, T6I4-65, and RRA conditions, (d) COD versus ΔK curves with achieved COD values at the moment of applied overload for the T7451, T6I4-65, and RRA conditions.	14
Figure 4 - (a) Pneumatic workbench, (b) fatigue results of pressurized samples.	15
Figure 5 - Crack tip length as a function of the number of cycles for the Alclad 2024-T3 alloy. The open symbols represent the base material and filled symbols after laser processing.	17
Figure 6 – Overview of the residual strength Test– ERJ-190.	18
Figure 7 – E-190 E2 wing lower skin crack growth and residual strength test.	19
Figure 8 – Comparison of SN behavior for Briles (IA) and HST11 (IB & IC) fasteners.	20
Figure 9 – Fuselage panel test set-up - general view.	21
Figure 10 - Riveted panel crack propagation results.	21
Figure 11 - Bonded panel crack propagation results.	22
Figure 12 - Semi wing fatigue test specimen and rig.	23
Figure 13 – FSW - Advanced upper wing cover concept.	24
Figure 14 - FML lower wing cover demonstrator.	24
Figure 15 - Complete setup for axial tests.	25
Figure 16 – Test results: (a) Relative position of fracture surface in the crack growth rate curve – axial (or mixed) mode of loading, (b) fracture surface for increasing crack growth rate for lap section – axial mode.	26
Figure 17 – Overview of CCS test specimen and FEM mesh.	28
Figure 18 – Selected FEM model results.	28
Figure 19 – Strain wave propagation along time.	28

Figure 20 – (a) Overview of the test specimens (curved laminate plates), (b) ABAQUS® analysis results - undeformed and deformed shape with 30mm crack.	29
Figure 21 – Comparison of numerical and experimental Energy Release Rate.....	30
Figure 22 – Predicted failure modes for stiffened composite panel.	31
Figure 23 – Load-displacement curve for panel impacted at different velocities.	31
Figure 24 - Jig developed for the fatigue tests based on Iosipescu method.	32
Figure 25 -S-N curves for the neat epoxy resin.....	33
Figure 26 – Embraer composite wing demonstrator – overview.	35
Figure 27 – (a) geometry of the lap-shear specimens (b) force -displacement curves for the best results for pin-less reference, four-and six-pin joints (c) and, average shear force for each type of joint.....	36
Figure 28 - FSpJ process without the addition of film interlayer. (1) sleeve plunging and plasticizing of the metal; (2) spot refilling and (3) joint consolidation.	37
Figure 29 – (A) Top view and (B) detailed view showing the spot area of a single lap Al	37
Figure 30 – (a) Composite and (b) metallic panels used for validation of LW experiments.	39
Figure 31 - Sensors and cables installed in an operator’s aircraft.	41
Figure 32 – Test Setup	43
Figure 33 - Aluminum 7049-T73 compact test sample (dimensions in inches): a) photography of test sample, b) sizes of test sample, and c) zoom of notch area.....	43
Figure 34 – Comparison between developed software (applying the Forman Theory in this case), DTA and test for (a) an average severity usage (b) a high severity usage.	43

INDEX OF TABLES

Table 1 – Comparison of results – from the example presented in Figure 1.....	10
Table 2 - SIF of each crack tip in original problem and relative difference between reference value and solution of splitting method – from the example presented in Figure 2.	10
Table 3 - Ageing heat treatment schedule for the T7451, T6I4-65 and RRA conditions	14

1. INTRODUCTION

This document was prepared to summarize fatigue and fracture investigations related to aerospace performed in Brazil during the past two years. Its contents will be presented during the 35th ICAF (International Committee of Aeronautical Fatigue) Conference to be held in Nagoya, Japan, in June 05 and 06, 2017. This is the second national review, and presently Brazil is a candidate country for the ICAF. Some of the research works presented are follow on activities from Ref. [1].

The following Brazilian institutions have collaborated during this period with research works on fatigue and fracture mechanics related to aeronautical products, and many of them have works added to this review:

- Brazilian Society of Engineering and Mechanical Sciences – ABCM – Rio de Janeiro - RJ
- Brazilian Air Force Aerospace Technological Center (CTA) – São José dos Campos - SP
- Institute for Technological Research (IPT) – São Paulo – SP
- University of São Paulo (USP) – Campus of São Carlos – São Carlos – SP
- University of São Paulo (USP) – Campus of Lorena – Lorena – SP
- State University of São Paulo (UNESP) – São José dos Campos – SP
- University of Campinas (UNICAMP) – Campinas - SP
- Federal University of Itajubá (UNIFEI) – Itajubá – MG
- Aeronautical Institute of Technology (ITA) – São José dos Campos – SP
- Embraer S/A – São José dos Campos – SP

Further, some works to be presented were developed in cooperation with foreign institutions, from which the following are mentioned here:

- TUDelft University of Technology– The Netherlands
- NLR – National Aerospace Laboratory – The Netherlands
- Helmholtz-Zentrum Geesthacht (HZG) – Germany
- Hamburg University of Technology (TCHH) – Germany
- University of Girona - Spain
- Sandia National Laboratories – USA

The author would like to thank to all partners from the Academy who have collaborated with this compilation, some of which will be cited during the report. The author is also grateful to Mr. Fernando F. Fernandez and to Dr. Giorgia T. Aleixo, from the R&D Department of Embraer, for their help and continuous support during the organization of this work.

2. ANALYSIS AND SIMULATION

There were two important contributions related to fracture analysis, whose partial results were already presented in Ref. [1]. These works were developed by the University of São Paulo under the supervision of Professor Sergio Proença.

Splitting Method in Multiple Site Damage – Mixed Mode Fracturing and Fatigue Problems (Ref. [2, 3])

This work was developed by I. Stoianov Cotta and Dr. S. Proença.

The Splitting Method is a decomposition method considered for mechanical modeling of multiple interacting cracks. Accordingly, the original problem is divided into a set of global and local sub-problems. The Generalized Finite Element Method (GFEM) is adopted aiming to find accurate numerical solutions for local sub-problems. Such problems are conceived to consider the stress concentration and the effects of interaction on the cracks.

The main contribution of this work is the combination of the Splitting Method and the GFEM/XFEM aiming at numerical modeling of the behavior of linear elastic domains with multiple cracks. The resulting computational framework for two-dimensional analysis described in the paper by its major features enables to consider different scenarios which have cracks with arbitrary polygonal shapes, cracks emanating from holes and internal cracks. Furthermore, mixed Modes I and II of crack openings can be considered. The original code in which the above mentioned computational framework was inserted is called SCIEnCE and was developed in Python® language, following an object-oriented approach. The crack tip driving forces are obtained by means of the computation of the J-Integral.

Figure 1 shows a numerical example, a solid with a crack attached to a hole and a slanted crack. The in-plane stress contours are presented for these two regions.

Table 1 presents a comparison of stress intensity factors in directions I and II for the developed framework (SCIEnCE) and Franc2D for the crack tips A, B and C (from Figure 1), where the Franc2D results were obtained with the J-Integral and the Displacement Correction Technique (DCT).

Splitting Method and Hybrid-Trefftz Formulation for Multisite Damage Analysis in Two-dimensional Domains (Ref. [4])

This work was developed by H. Argolô and Dr. S. Proença.

The aim of the work is to present a new strategy for multiple-site damage analysis by combining the splitting method and hybrid-Trefftz stress formulation in a two-dimensional domain. The first is a decomposition method originally conceived to obtain the solution of a cracked solid. Accordingly, the given problem is split into three subproblems: an uncracked global problem ($P_G^{(0)}$), a local problem ($P_L^{(k)}$) considering a single crack located in a reduced domain and a global problem ($P_G^{(k)}$) aiming to

account for the relative interaction effects among all the cracks. Most subproblems are independent and the solution results from a non-iterative strategy, which is one of the main benefits of this method. The hybrid-Trefftz stress formulation is a non-conventional finite element method where stresses and displacements are approximated, independently, in the domain and boundary of the element, respectively. The stress fields are hereby approximated by a basis function that solves the Navier equation and includes analytical fracture mechanics functions, so that the values of stress intensity factors are computed from the solution of the linear system. The hybrid-Trefftz formulation is used in the local problem $P_L^{(k)}$ of the splitting method, therefore improving the performance of the method and providing accurate solutions with very coarse meshes.

Finally, it is shown through the numerical examples that the splitting method and hybrid-Trefftz formulation framework proposed allow conducting accurate analysis. Once exploring a parallel processing, taking advantage of the independence of each subproblem, the framework can be extended to consider different scenarios of multisite cracked solids with a low computation cost.

As part of the numerical applications presented in the work, Figure 2 shows a case where three cracks and four holes are placed in a rectangular domain of a solid under traction. The global problem $P_G^{(0)}$ is illustrated as an example. The comparison with reference stress intensity solutions (obtained with Ansys®) is presented in Figure 2.

Table 1 – Comparison of results – from the example presented in Figure 1.

	Crack tip A		Crack tip B		Crack tip C	
	K_I	K_{II}	K_I	K_{II}	K_I	K_{II}
SCIEnCE	2.820	0.0280	1.264	0.968	1.248	0.973
Franc2D (DCT)	2.815	-0.0219	1.248	1.013	1.201	1.018
Franc2D (J Integral)	2.815	-0.0241	1.255	0.967	1.208	0.978

Table 2 - SIF of each crack tip in original problem and relative difference between reference value and solution of splitting method – from the example presented in Figure 2.

SIF	Solution of splitting method				Reference value			
	Tip1	Tip2	Tip3	Tip4	Tip1	Tip2	Tip3	Tip4
K_I	0.896	0.885	0.885	0.896	0.897	0.875	0.875	0.897
K_{II}	0.848	0.837	0.837	0.849	0.864	0.847	0.847	0.864
Relative difference (%)								
K_I	0.114	1.124	1.137	0.119				
K_{II}	1.798	1.173	1.178	1.178				

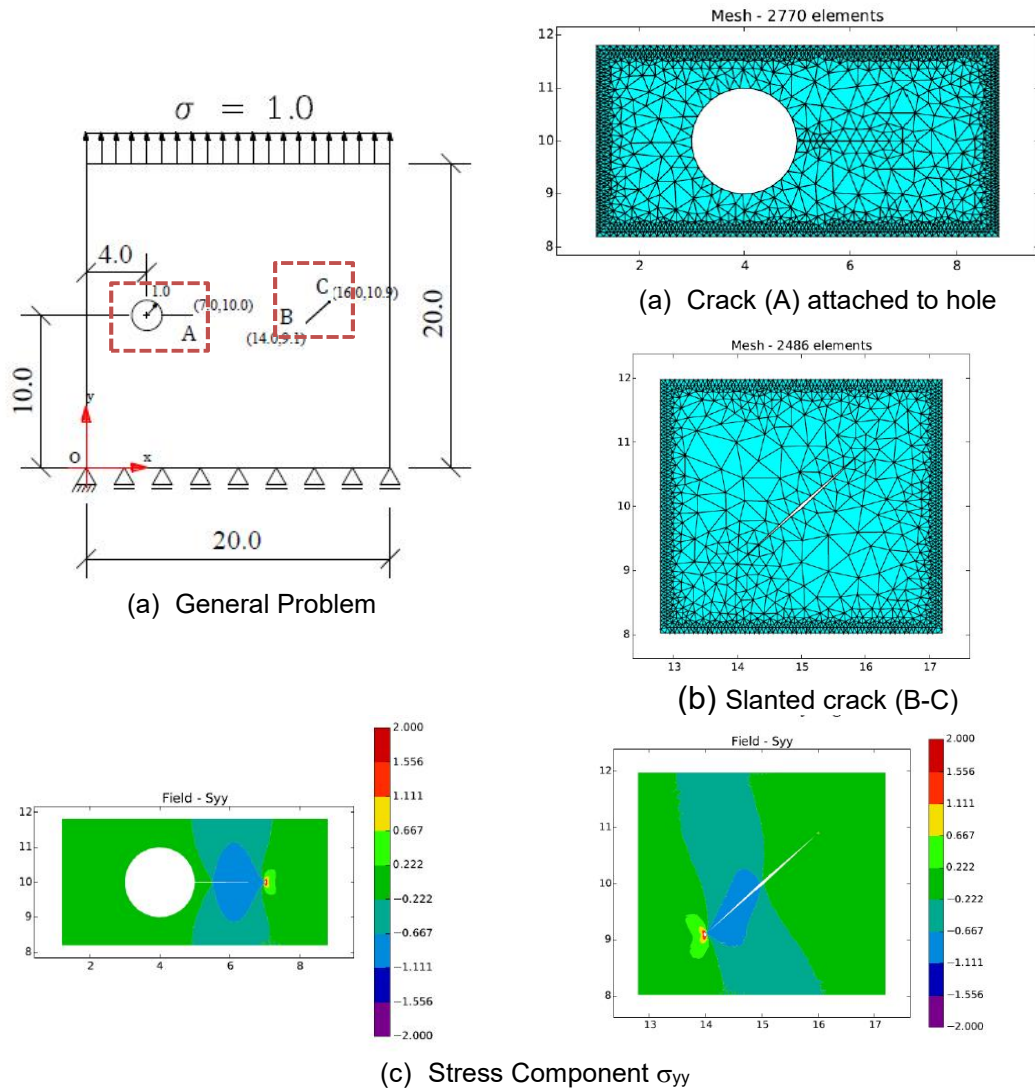


Figure 1 – Splitting method - numerical example.

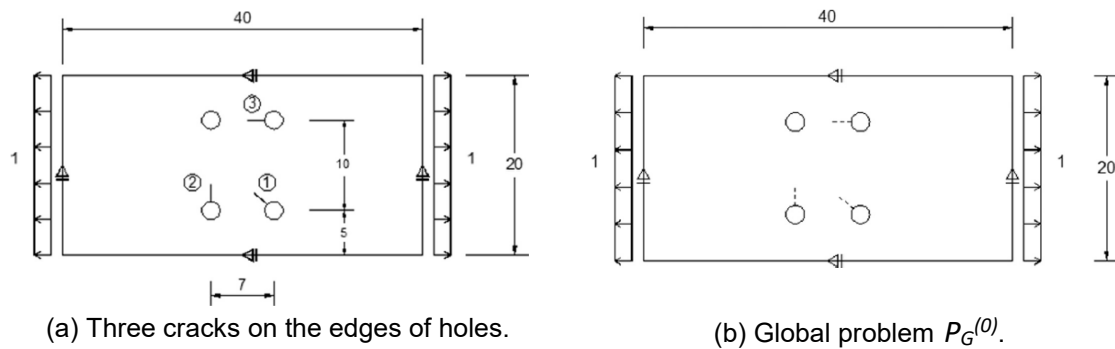


Figure 2 – Example of application – three cracks on the edge of holes.

3. METALLIC MATERIALS – FATIGUE AND FRACTURE PROPERTIES

Some important works with metallic materials fatigue properties have been developed by Dr. Waldek B. Filho and his team, from the Department of Materials Engineering, University of São Paulo (USP), and by Dr. André L. M. Carvalho, from the University of Ponta Grossa (UEPG).

Microstructural Analysis, Fracture Toughness and Fatigue Life of AA7050-T7451 and AA2050-T84 Alloys (Ref [5])

The motivation of this study was the substitution of AA7050-T7451 by AA2050-T84 for application in typical aeronautical structures, e.g., spars in vertical tail, ribs, and frames. This substitution becomes attractive because AA2050-T84 presents lower density, higher elastic modulus and better damage tolerance behavior. A comparative study was made of the AA7050-T7451 and AA2050-T84 alloys and of the L-T and T-L directions, and the behavior of these alloys when subjected to room and cryogenic temperatures was also analyzed. Comparative analyses of the alloys and directions were performed using fatigue-precracked compact tension C(T) test specimens. The behavior of the alloys was analyzed based on fracture toughness, K_{Ic} , K-R curve, fatigue and FCG tests. Their microstructure was characterized by optical microscopy, scanning electron microscopy and transmission electron microscopy. The K-R curve indicated that resistance to crack propagation was higher in the L-T direction than in the T-L direction at room temperature. In a comparison of the two alloys in the L-T direction at room temperature, they were found to present similar stress intensity factors under similar loading conditions. The results of the fatigue tests demonstrated that the T-L direction is more sensitive to the load ratio for AA2050-T84. An analysis of the results in the L-T and T-L directions indicated that the two alloys exhibited anisotropic behavior.

This is a follow-on work from the one presented in Ref. [1]. More details about the work will be presented during the ICAF Conference in Nagoya, Japan.

Effect of Interrupted Ageing and Retrogression-Reageing Treatments on Fatigue Crack Growth with a Single Applied Overload in 7050 Aluminum Alloy (Ref. [6])

This work was developed by André L. M. Carvalho and Juliana P. Martins (UEPG).

The influences of interrupted ageing (I = interrupted) and retrogression and re-ageing (RRA) heat treatments on fatigue crack growth with a single applied overload in 7050 aluminum alloy were investigated in this work. The main aims were to evaluate the influence of these heat treatment conditions on tensile properties, mainly fatigue crack growth rate and fracture process in the low–moderate ΔK region; to determine how both T614-65 and RRA ageing treatments generate bimodal microstructure features as a contribution of the two conditions on the crack closure phenomenon; and the influence of the single applied overload to fatigue crack growth retardation. The results

show that by using the RRA heat treatment condition it is possible to enhance the ductility without detrimental effects on the yield stress. T6I4-65 and RRA conditions contributed to enhancement of the crack closure phenomenon in the low–moderate ΔK region, and, accordingly, produced a lower fatigue crack growth rate in relation to the traditional T7451 condition.

Table 3 shows the two types of heat treatment considered in the present study, carried out per the following schedules. The other condition considered for reference was the as-received T7451 condition.

Figure 3 shows the outline of the test specimens and some selected results from this investigation, such as the dadN vs. ΔK curves for the three aged conditions, the COD vs. ΔK trends for T7451, T6I4-65, and RRA conditions and the COD versus ΔK curves with achieved COD values by the time that the overload was applied for the T7451, T6I4-65, and RRA conditions.

4. METALLIC MATERIALS – PROCESSES

Regarding metallic material processes for titanium and aluminium alloys, during this period two contributions were supplied.

Fatigue in Laser Welded Titanium Tubes intended for use in Pneumatic Systems: Statistical Analysis (Ref. [7])

This work was developed in partnership between the University of São Paulo (Dr. Sheila M. de Carvalho and Professor Carlos Baptista) and DCTA (Dr. Milton Lima).

The pneumatic system conducts the pressurized hot air from the engine to the environmental systems of aircrafts. Considering the severe operating conditions to which the pneumatic system is subjected, which include pressurization and heating cycles, the employed materials and manufacturing processes must be adequately selected. Titanium alloys are suitable materials for use in this system due to their elevated temperature fatigue and oxidation resistance. A number of in-flight failures of titanium ducts, all of them associated to cracking adjacent to welds, have been reported in literature. The failure propensity by thermo-mechanical cycling doesn't mean that there are recurring failures of this system. However, one should consider this possibility before an accident occurs, which could lead to the aircraft crash with human and material losses. In order to provide information concerned with the service performance of the titanium ducts, a pneumatic workbench, Figure 4 (a), capable of reproducing the temperature and pressure cycles found in flight conditions was developed in a previous work.

Table 3 - Ageing heat treatment schedule for the T7451, T6I4-65 and RRA conditions

Condition	Solution heat treatment	Ageing	Reversion treatment	Re-ageing treatment
T7451		As received		
RRA	758 K (485°C) for 4h	Ageing at 403 K (130°C) for 24h	Reversion at 458 K (185°C) for 20 min	Re-ageing at 338 K (65°C) for two months
T6I4-65		Ageing interrupted at 403 K (130°C) for 15 min		Ageing at 338 K (65°C) for two months

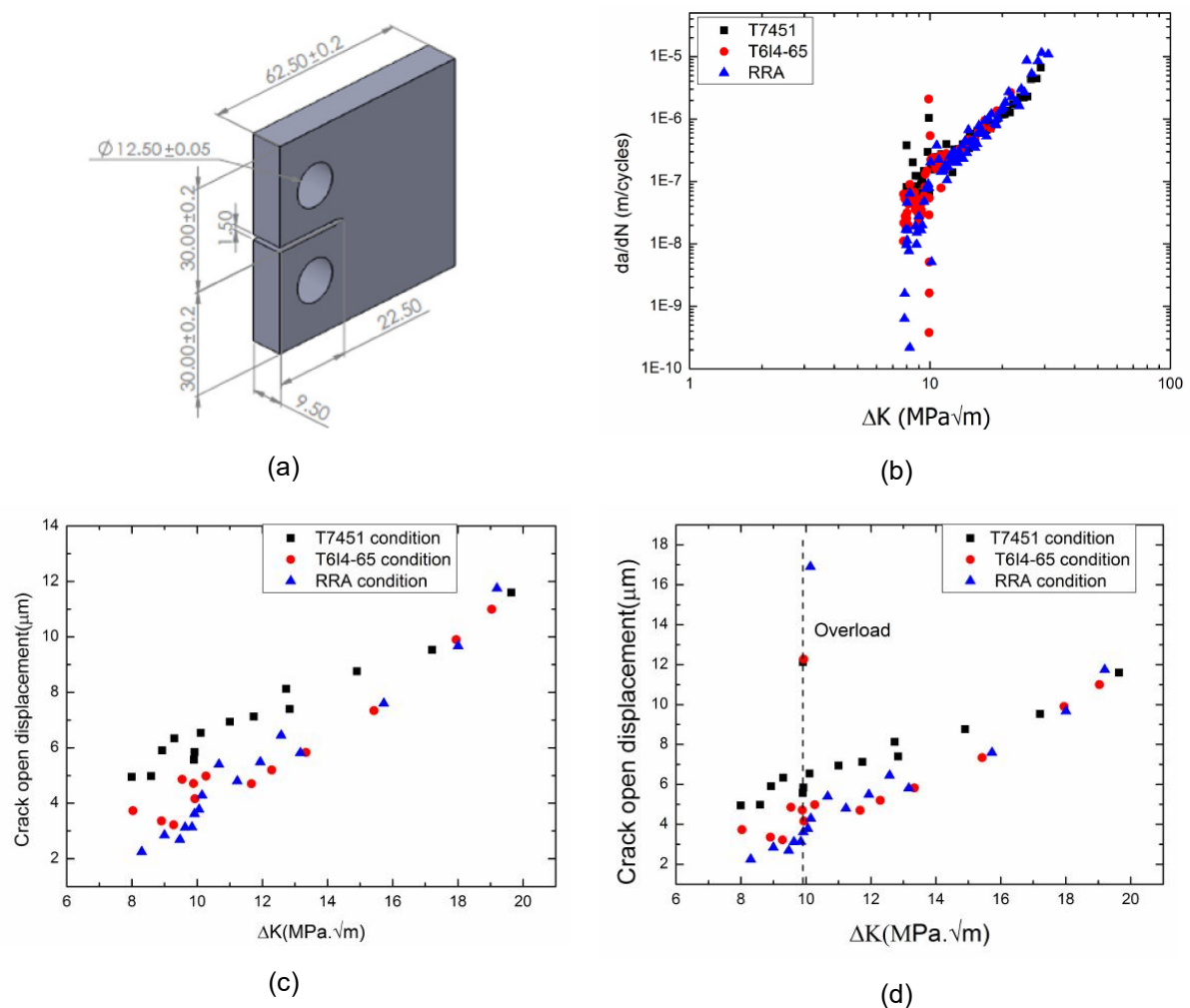


Figure 3 – Selected results from Ref. [6]. (a) geometry of the compact tension Al alloy specimen (dimensions in mm), (b) fatigue crack growth rate versus ΔK curves for the three aged conditions, (c) COD in the function stress intensity factor, ΔK , from the T7451, T6I4-65, and RRA conditions, (d) COD versus ΔK curves with achieved COD values at the moment of applied overload for the T7451, T6I4-65, and RRA conditions.

By simulating the operational conditions in titanium parts welded by the Tungsten-Inert Gas (TIG) process, it was observed that some ducts failed after a number of pressurization cycles below the expected service life. These failures have driven further development of laser beam welding as an alternative method. A fiber laser with 2 kW power had been employed to weld commercial purity titanium tuber with 0.5 mm wall thickness and 50 mm diameter. Ring-shaped specimens were employed to assess the fatigue performance of the laser beam and TIG welded tubes after service cycles simulation, Figure 4 (b).

In this work, the Analysis of Variance (ANOVA) of the previously obtained data was performed in order to compare the fatigue characteristics of the base material to the laser and TIG welded tubes, before and after the pressurization cycles. The variances of $\log(N_f)$ exhibit Normal behavior, which means that Bartlett's test is more suitable to the analyses. The results demonstrate that the hypothesis that the variances are the same for the various stress levels can not be refuted. Thus, the Analysis of Variance is suitable to assess significant lifetime differences between the tested conditions. By considering a 2-Way Analysis of Variance, it was verified that both the stress level and material condition are significant variables on the average fatigue life. The Turkey test results were employed for comparison of the workbench-cycled samples and showed that the TIG welded tubes have an average lifetime lower than the un-welded and laser welded ones. On the other hand, the fatigue results of the non-pressurized samples indicated that no significant differences exist between TIG and laser welds. One possible physical reason for these differences between pressurized and non-pressurized conditions is that the defects present in 2 TIG weld beads are more susceptible to develop into micro-cracks during elevated temperature pressurization in workbench, thus resulting in lower fatigue resistance than the laser welds.

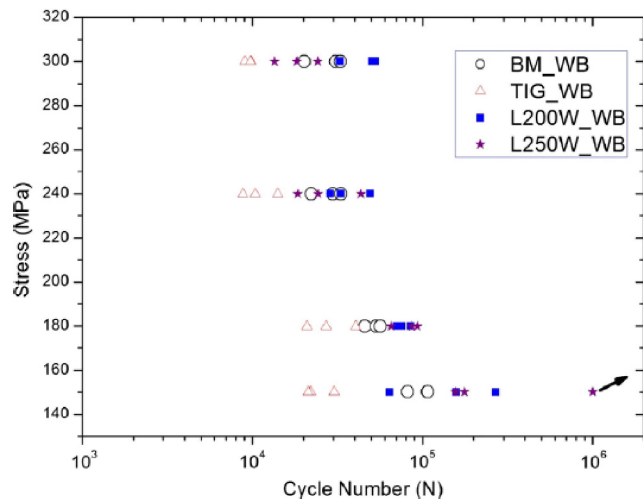


Figure 4 - (a) Pneumatic workbench, (b) fatigue results of pressurized samples.

The Influence of Laser Surface Treatment on The Fatigue Crack Growth of an Aluminum Alloy Sheet (Ref. [8])

This work was developed by Maurício C. da Cunha (Embraer) and Dr. Milton Lima (DCTA).

It is known that compressive residual stresses enhance the performance of structural components by retarding the crack propagation rate, extending the fatigue life of such components. For this reason, aircraft manufacturers often apply processes like shot peening, ball-burnishing and more recently laser shock peening to improve the fatigue life of structural parts. Recent studies of a new process that use local heating for introduction of residual stress, have shown good results on the retardation of fatigue crack growth.

The purpose of this work is to study the effect of local heating using the laser as a surface treatment to introduce compressive residual stress and retard the crack propagation of aluminum alloy sheets. Some process parameters as laser speed, number of heating lines and surface pre-treatment are changed in order to obtain process conditions which primarily act on the residual stress field due to rapid heating and cooling. The local heating process was performed over 1.6 mm thickness aluminum sheets of an Alclad 2024-T3 alloy, with one or two heating lines generated by a defocused Yb-fiber laser and operated continuously.

The defocused laser beam generated a laser spot diameter of 2 mm to introduce heating, but avoid melting the aluminum alloy. For crack propagation tests, modified C(T) specimens were manufactured and tested according to ASTM E647 procedure. The laser power of 200 W was used and the laser speed was varied between 1 and 50 mm/s. Also, one and two heating lines were irradiated and for some specimens a layer of black graphite was applied over the surface. The results obtained showed that the fatigue crack growth was retarded and the fatigue life was increased. The best results were obtained from specimens with black graphite applied previously to the laser irradiation combined with two laser heating lines. Figure 5 illustrates the enhanced lifetime of the coupons after fatigue crack growth tests. The original 2024 alloy (open symbols) showed a life around 67,000 cycles and the lasered 2G (two lines with graphite coating) presented a life of about 105,000 cycles.

In conclusion, it was demonstrated the local heating process using a defocused Yb-fiber laser has the potential to be used for crack growth retardation of aerospace aluminum alloy sheets.

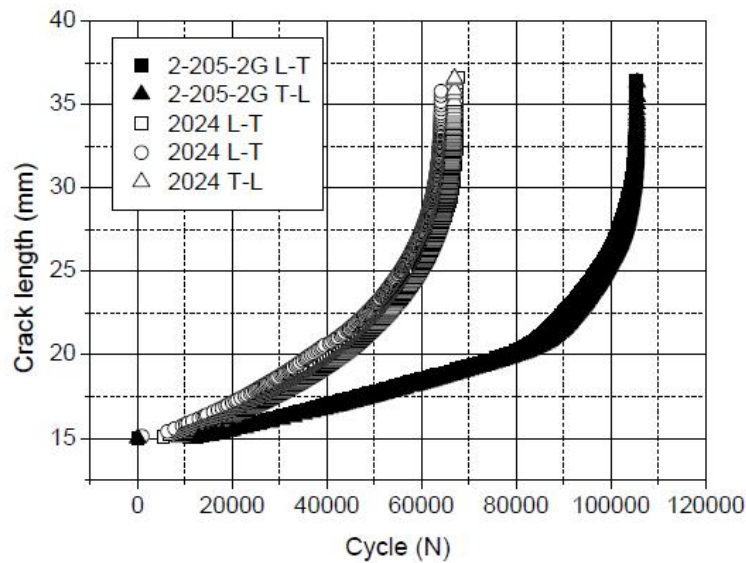


Figure 5 - Crack tip length as a function of the number of cycles for the Alclad 2024-T3 alloy. The open symbols represent the number of cycles obtained for the baseline material and the filled symbols represent the number of cycles obtained after laser processing.

5. METALLIC MATERIALS – STRUCTURES

During the period 2015-2017, there were important activities related to development and certification of regional and military aircraft. Additionally, there were advances in tests for demonstrators of new materials and technologies.

Embraer 170/175/190/195 E1 (First Generation)

In the first half of 2016, Embraer 170 (ERJ-170) and Embraer 190 (ERJ-190) complied with Part 26 Subpart C (WFD and LOV) Requirements. Embraer methodology for WFD was approved by the FAA/ANAC in the second half of 2015. Most of the WFD susceptible structures were assessed via Full-scale Fatigue Test and demonstration of the structure residual strength. The full-scale fatigue tests for both models were extended to three lifetimes. Both test specimens reached 240,000 pressurized flight cycles by 2014. The residual strength tests were performed from the end of 2014 to the first half of 2015. Certain WFD susceptible structures for which the residual strength test did not provide the required load (mainly for derived models) had their residual strength demonstrated by teardown inspections. Similarly, some WFD susceptible structures for which three lifetimes were not reached during the test (usually because these structures were not well represented) had their residual strength demonstrated by analysis. Figure 6 shows an overview of the residual strength test for ERJ-190.



Figure 6 – Overview of the residual strength Test – ERJ-190.

Embraer 190/195 E2 (Second Generation)

Currently there are two new products under development for Embraer Commercial Aviation, ERJ-190 E2 and ERJ-195 E2. These products are re-engined versions of the E-Jets, powered with PW1900G turbofan engines, that lead to significant gains in performance.

The new engines and the increased performance requirements led to the necessity of new wing, empennage, pylon and landing gear designs, and to some modifications in the fuselage design. The ERJ 190 E2 prototype had its first flight in May 2016, and the ERJ 195 E2 prototype first flight occurred in March of 2017.

Due to the modifications above mentioned (including new materials, design and manufacturing methods), these products are being subject to a new development and certification campaign. The static tests for ERJ 190/195 E2 are underway, and the Full-scale fatigue test is expected for the second half of 2017. The candidate LOV for both new aircraft is 80,000 FC, that is the same as for the first generation of E-Jets.

There is a wide range of development and certification tests being performed for the ERJ 190/195 aircraft, such as material tests, subcomponents and component tests and full-scale fatigue tests, for the full fixed structure, empennages, landing gears, control surfaces, etc.

As an example, Figure 7 shows the overview of the crack propagation test performed for a panel of the ERJ 190 E2 wing lower skin.



Figure 7 – E-190 E2 wing lower skin panel crack propagation tests.

Subcomponent and Component Tests – Lap / Butt Joints (Ref. [9])

A study on the simulation of riveted joints using 3D finite elements and contact tools, as analytic contact, to improve the results accuracy, was described the previous review (Ref. [1]). The main objective of that work was to recommend best practices to conduct a 3D FE analysis of a riveted butt joint configuration, and to identify which parameters and effects must be considered to reach accurate and reliable results.

Such work was performed through a cooperation project between IPT and Embraer, and continued with an experimental work for a series of joint configurations. The majority of specimens tested correspond to single strips. Some selected results are presented in this report. Figure 8 (from Ref. [9]) shows the comparison of SN curves for specimens with two joints for the same material (Al 2524-T3), same thickness (1.6mm for the skin and 2.0mm for the splices), same fastener diameter (3.96 mm), but with two countersunk fastener types, Briles and Hi-Lite (HST11). It is interesting to observe the differences in fatigue behavior for high cycle and low cycle fatigue, that is attributed mainly due to differences in fastener flexibility.

Another interesting result showed in this figure is the change of failure from the skin to the splice as long as the stress level decreases (i.e., for high cycle).

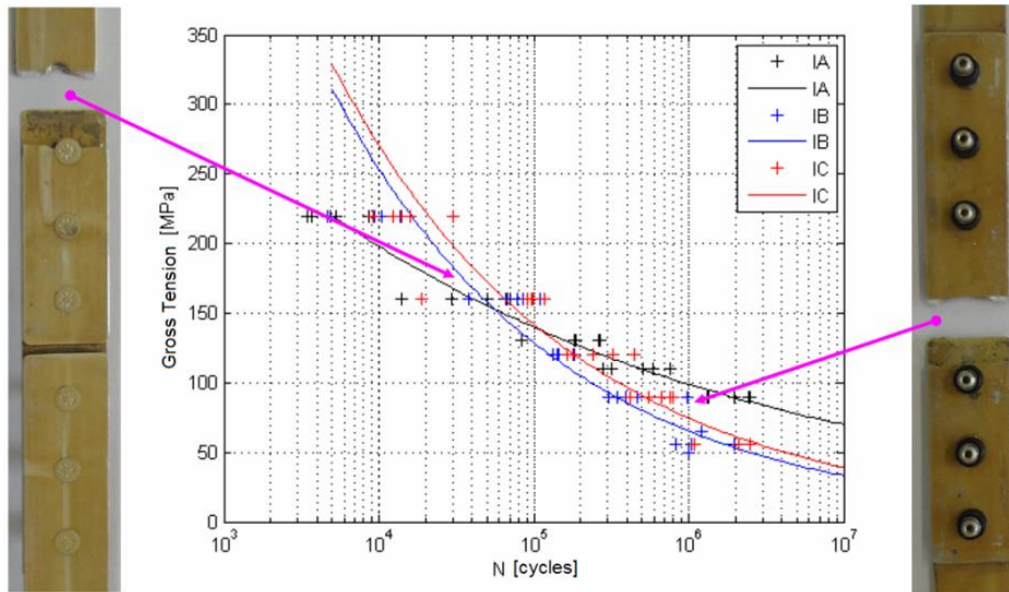


Figure 8 – Comparison of SN behavior for Briles (IA) and HST11 (IB & IC) fasteners.

Fuselage Panel Tests

The fuselage panel tests are part of a Research and Development cooperation project between Embraer and ITA. The purpose of the work is to investigate the application of modern technologies, such as bonding and FML.

The results of crack propagation and residual strength tests of fuselage panels in four configurations are presented: riveted panels (baseline), bonded panels, FML skin panels, and FML strap reinforced panels. Those panels were designed and manufactured by Embraer, and instrumented and tested at ITA laboratories. Each panel has five stringers, and the initial damage scenario is a central stringer failed and a 12mm skin crack. After a complete two-bay crack was reached, each panel was tested up to its failure.

Additionally, analysis was performed with finite element models and strain energy release rate method for stress intensity factors computation, as well as analytical methods from the literature. The analysis methods currently applied by Embraer resulted in good correlation with tests results for the riveted panels. For modern technologies, the combination of current and new methods provided satisfactory results too. Regarding the residual strength tests, high load redistribution along the joint of intact adjacent stringer to skin was observed without failure. FML showed superior performance when compared to the baseline panel, showing great potential for future applications.

Figure 9 shows an overview of the test setup. Some test results are presented in Figure 10 and Figure 11. Due to the very high stiffness of the bonded joint, a failed stringer will result in higher local stress concentration in skin, and consequently faster crack propagation than in baseline riveted panel, as observed in Figure 11.

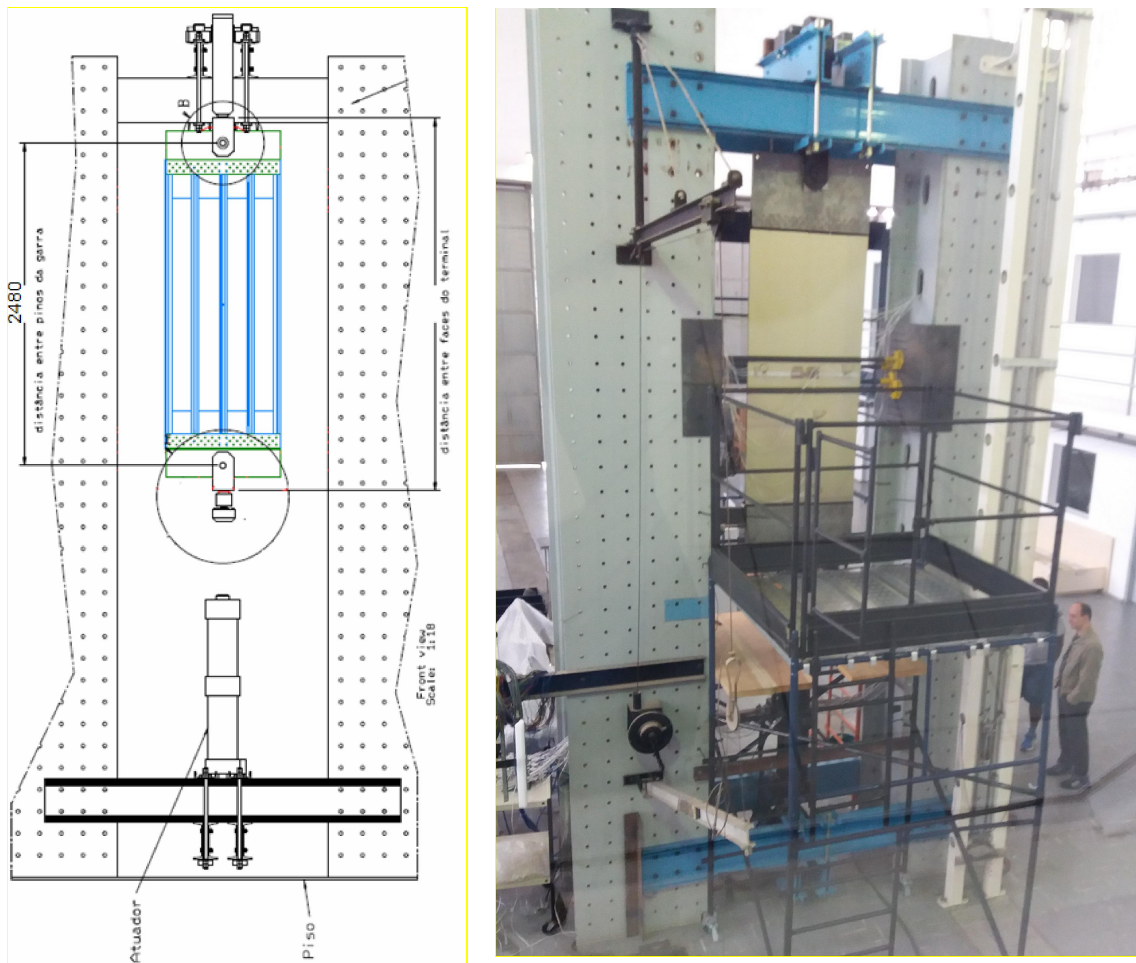


Figure 9 – Fuselage panel test set-up - general view.

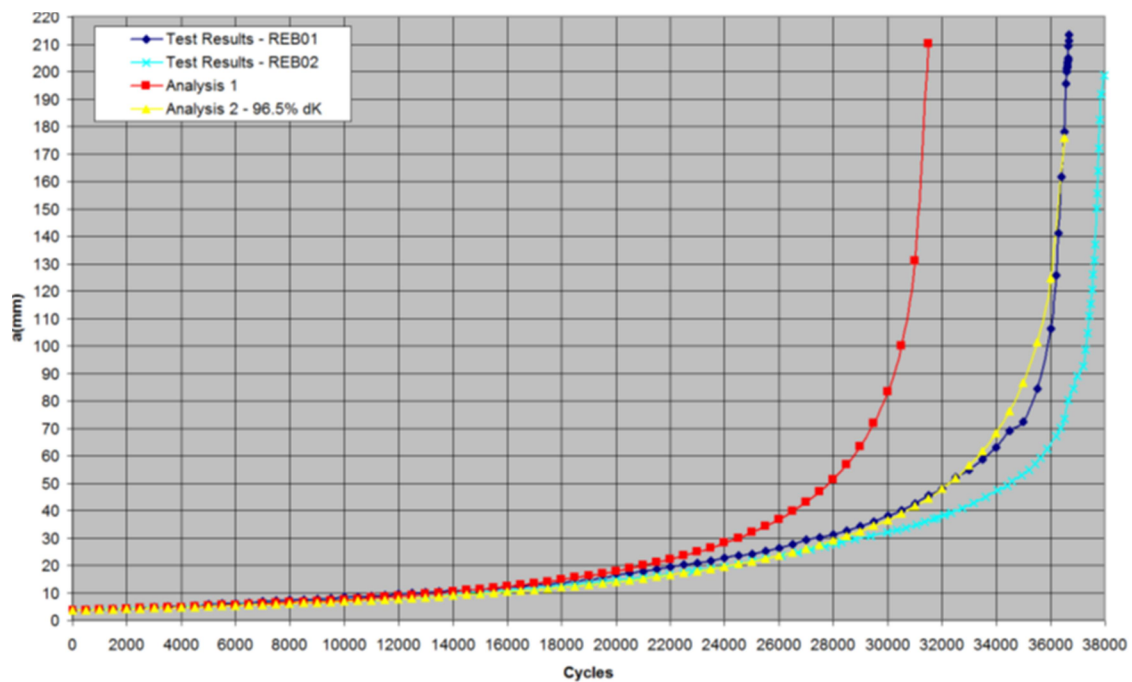


Figure 10 - Riveted panel crack propagation results.

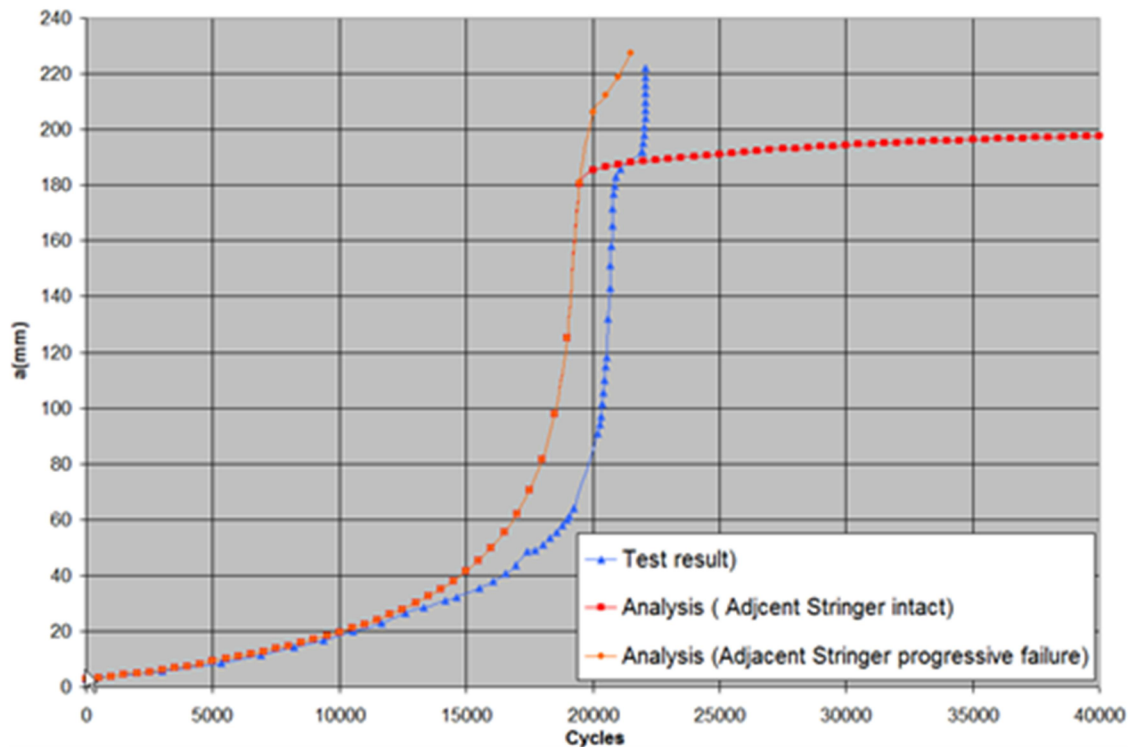


Figure 11 - Bonded panel crack propagation results.

Wing Demonstrator

In terms of application of recent technologies for specific aircraft structural components, some details about a fuselage demonstrator including novel technologies such as FSW and FML and subject to a range of static and fatigue tests were presented in Ref. [1]. Besides this R&D activity, during the last years a set of static and fatigue tests were performed for a configuration corresponding to a typical semi wing of a regional aircraft.

The main technologies included in this wing demonstrator were: Friction Stir Welding (FSW), Structural Bonding and Fiber Metal Laminate (FML). FSW was applied in an advanced wing spar, presented in the last ICAF Report (Ref. [1]), and also in an advanced upper wing cover, for which a more detailed explanation will be presented in this review. FML and Metal Bonding were applied to the lower wing cover, and the summary of these applications will be also presented here.

Currently, the fatigue test specimen has been subjected to a complex wing spectrum loading condition for a test period corresponding to three lifetimes of a typical regional aircraft, such as ERJ-145. Figure 12 shows an overview of the semi wing fatigue test specimen and rig.

One concept being evaluated by the R&D department is an advanced upper wing cover with parts welded with FSW technology. This concept was presented by Constellium and Embraer during the AEROMAT Conference in 2014 (Ref. [10]). Some advantages of this concept are the optimization of buy to fly, means of reducing manufacturing

costs etc. Figure 13 shows the parts comprising two different thickness aluminium alloys successfully welded. All plates are made of plate AA7449-T7951 that presents superior static properties when compared to most conventional aircraft aluminium alloys. These two sub-component demonstrators were assembled to a wing structure and currently have been subjected to service loads conditions for verification of their fatigue and crack growth performance.

For a long time in the aircraft structures, the primary components were constituted mainly of aluminum alloys. However, Fiber Metal Laminates (FML) exhibit excellent damage tolerance (i.e., crack growth and residual strength) performance, while preserving similarity with aluminum structures. As the average aircraft economic life is over 30 years and there are new perspectives of extending this lifetime, the inspection and maintenance costs are becoming more important design drivers.

An FML lower wing skin would be a suitable candidate to improve the performance of the fatigue loading dominated lower wing. For this reason, Embraer is currently investigating the application of FML in this primary structure.

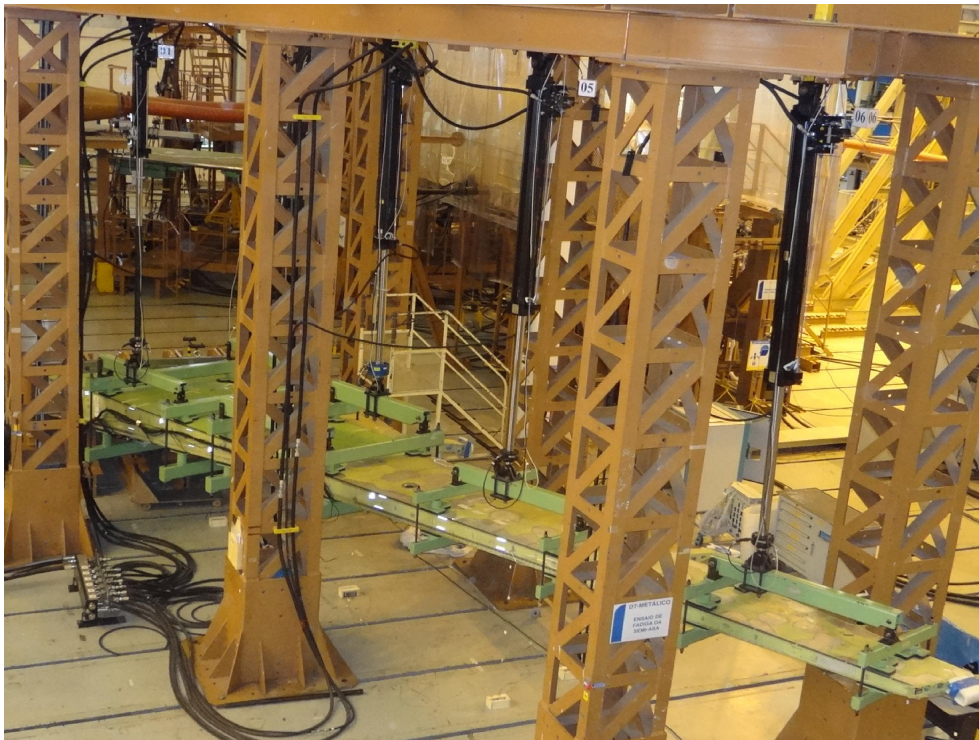


Figure 12 - Semi wing fatigue test specimen and rig.

The development of the Lower Wing Cover Demonstrator (Figure 14) was carried out in cooperation with Arconic. It consists of AA2524-T3 aluminum sheets alternately bonded to uni-directional fiber glass plies embedded in adhesive system layers. Feasible manufacturing routes are required in order to apply FML in large and complex curved structures such as lower wing panels. The investigation and development of manufacturing processes for FML has been part of the Embraer's strategy for developing the TRL on this technology for structural applications. This lower wing cover

has been assembled into the full semi-wing demonstrator. The semi-wing is being tested at Embraer under service conditions.

The lessons learned from this new material application may influence the future developments of optimized FML structures concepts.

This concept was presented by Embraer during the AEROMAT Conference in 2017 (Ref. [11]).

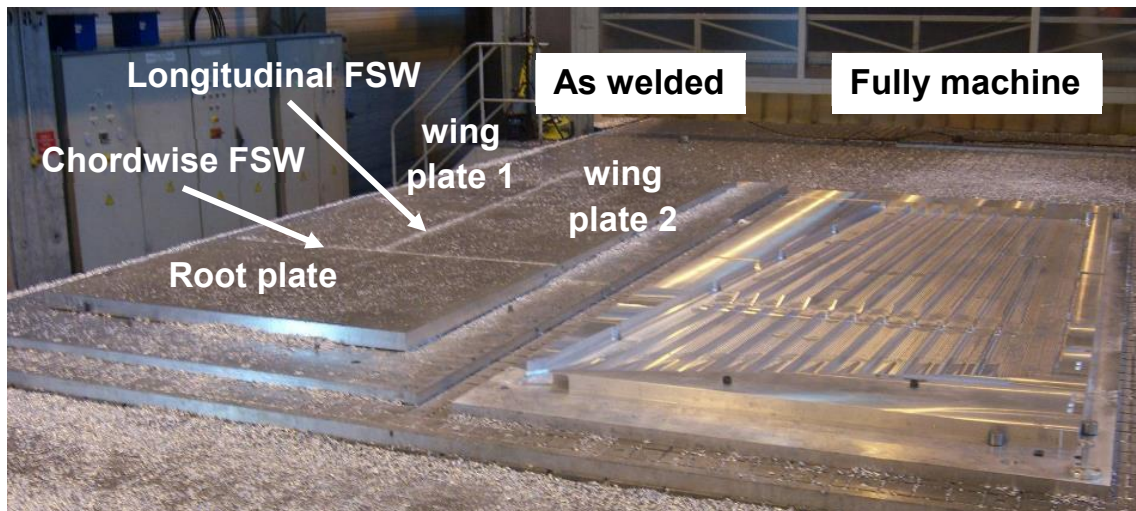


Figure 13 – FSW - Advanced upper wing cover concept.

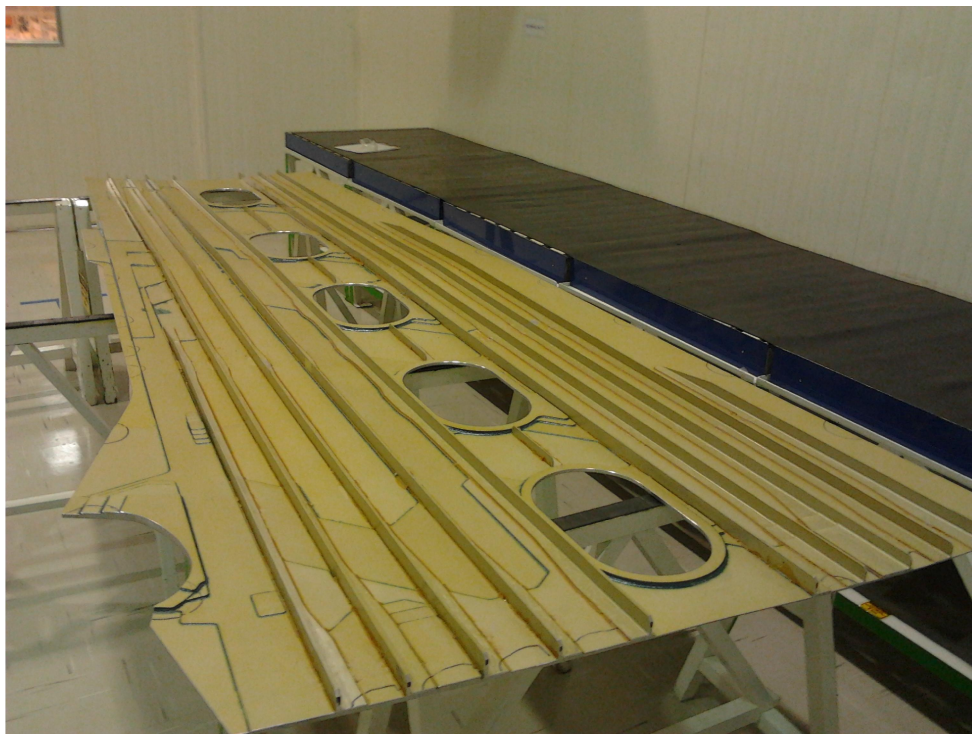


Figure 14 - FML lower wing cover demonstrator.

6. COMPOSITE MATERIALS

During the last two years, there were important contributions from the Aeronautical Institute of Technology (ITA), from the Department of Aerospace Science and Technology (DCTA) and other partner institutions, as presented below.

The Relationship Between Pure Delamination Modes I and II on the Crack Growth Rate Process in Cracked Lap Shear Specimen (CLS) of 5 Harness Satin Composites (Ref. [12])

This work was developed by Marcos Y. Shiino (UNESP), by Dr. Maurício Donadon and co-workers. It was preceded by another paper that was addressed during the last Brazilian Review (Ref. [13]).

Carbon fiber reinforced polymer (CFRP) structures can include dropping-off plies in order to comply with design requirements aiming at significant weight savings. However, this type of discontinuity represents a potential source of delamination initiation and propagation which requires assessment of the mechanisms acting at the crack tip.

This research investigates the influence of delamination modes I and II on the overall damage process observed in CLS specimen subjected to cyclic loads. The main contribution of the work focuses on the identification and physical interpretation of complex failure mechanisms in harness satin fabric. For this purpose, a detailed fractographic analysis was carried out to qualitatively assess the surface fractures in these types of laminates. Results obtained for cyclic loaded CLS specimens were compared to analytical closed form solutions available in the literature. The results indicated that delamination front exhibited distinguishable delamination modes I and II propagating at constant mixed mode ratio (G_I/G_T).

Figure 15 shows the test setup, including a universal testing machine and strain gages used to correlate the crack length with changes in compliance.

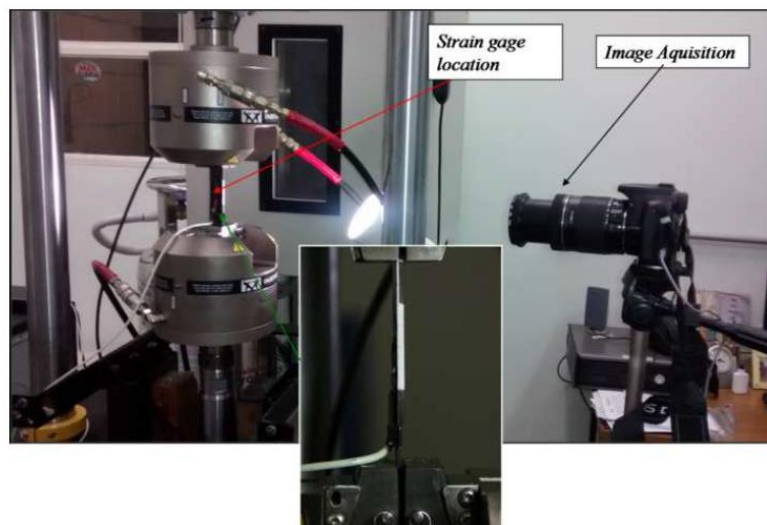
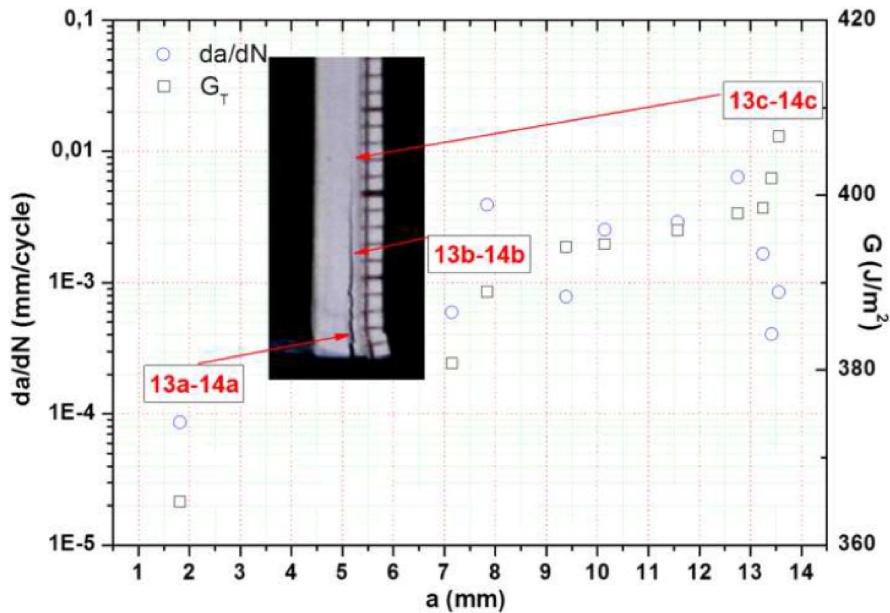
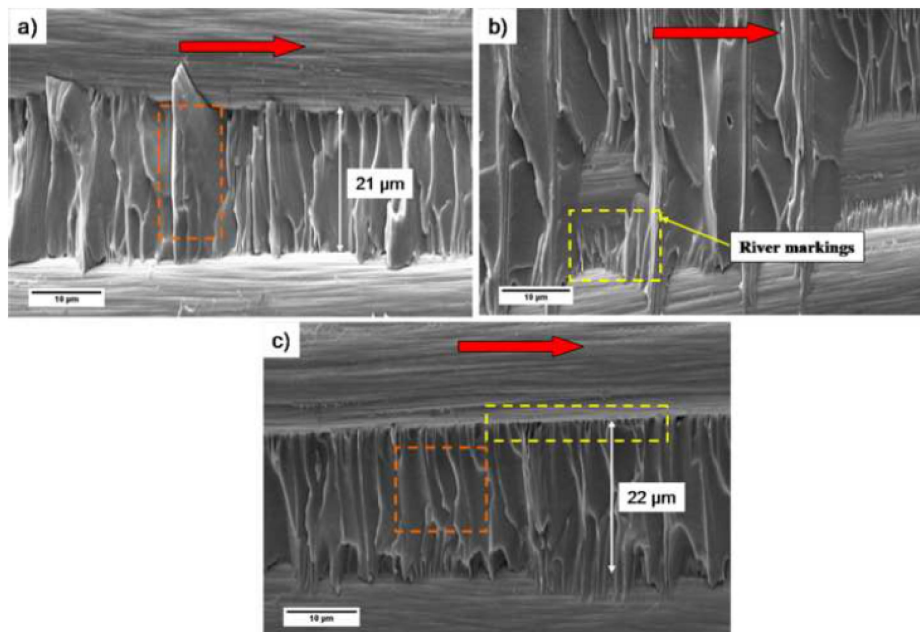


Figure 15 - Complete setup for axial tests.

The crack propagation rate da/dN was obtained from the tests for Mode I, Mode II and for axial (mixed) mode. Figure 16(a) shows, as an example, the crack growth rate curve for the axial mode of loading. Figure 16(b) shows one example of fractographic analysis the fracture surface for increasing crack growth rate for the lap section under axial mode.



(a)



(b)

Figure 16 – Test results: (a) Relative position of fracture surface in the crack growth rate curve – axial (or mixed) mode of loading, (b) fracture surface for increasing crack growth rate for lap section – axial mode.

A Numerical Study on Testing Configurations for Intralaminar Fiber Kinking Fracture Toughness Characterization of Composites in The Dynamic Regime (Ref. [14])

A Numerical Study on Testing Configurations for Intralaminar Tensile Fracture Toughness of Composites in The Dynamic Regime (Ref. [15])

These two investigations are complementary, and were developed by two MsC students under supervision of Professor Mauricio Donadon (ITA).

Composite aerostructures are subjected to different impact loads, which may induce intralaminar damage, compromising the aircraft safety. The understanding of the mechanical behavior of the composite material when subjected to extreme dynamic loadings is a very important issue.

These two papers present numerical studies of testing configurations for intralaminar fiber kinking fracture toughness characterization of composite laminates subjected to high strain rates. Standard test methods have not been found for this kind of experiment. Therefore, specimens with different geometries and layup configurations were considered in the numerical studies in order to define an optimum testing configuration for these types of tests.

The simulations were carried out using a continuum damage mechanics based failure model implemented into user subroutine VUMAT within ABAQUS® software. The proposed optimum testing configurations are intended to be mounted in a Split Hopkinson pressure bar facility. Finally, comparative studies showing the advantages and disadvantages of each testing configuration studied were presented and conclusions were drawn.

The FE model was discretized using C3D8 solid elements available in ABAQUS®. The layers were assumed to be made plain weave woven carbon fabric. Details about the material properties are found in the references.

Both specimen configurations have a $[0/90]_{7s}$ lay-up and each ply has a thickness of 0.25mm. Three configurations were evaluated: (a) SENB (single edge notched in bending), (b) DEN (double edge notched) and (c) CCS (compact compressive specimen). For this report, some information was selected from the CCS specimens.

Figure 17 shows the overview of the test specimen and the 3D FEM model created to represent it. An initial velocity of 15 m/s was applied to the striker. Virtual gages were positioned in the middle of the bars to obtain the strain pulses in the bars, and to verify if the signals are measurable. Also, it was verified how long the event lasted before the failure in compression takes place during the crack propagation.

Figure 18 shows the stress fields and the damage pattern. Figure 19 shows the predicted strain wave pattern for this specimen. The total time of the event was 47 μ s.

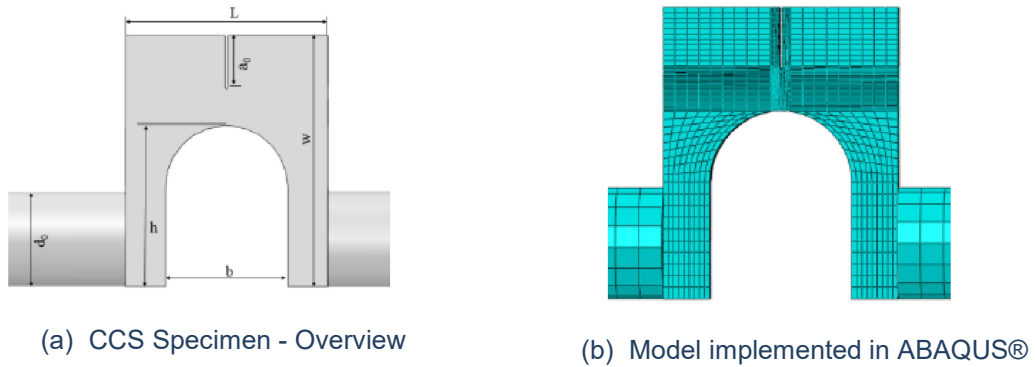


Figure 17 – Overview of CCS test specimen and FEM mesh.

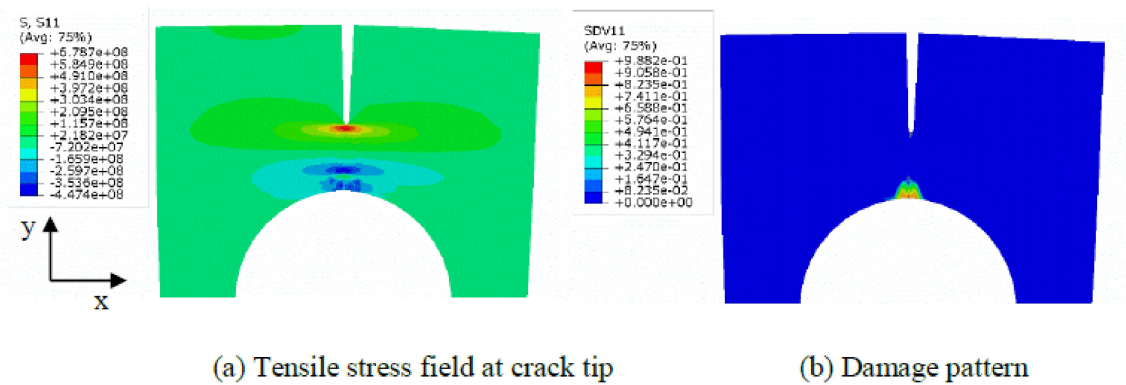


Figure 18 – Selected FEM analysis results.

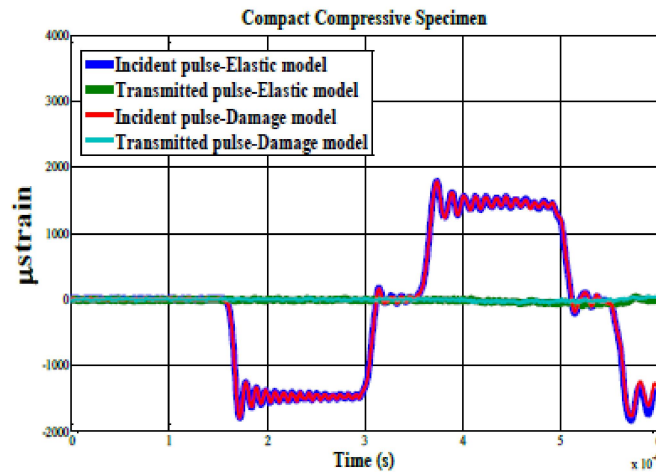


Figure 19 – Strain wave propagation along time.

A dedicated experimental work for validation of these results is expected to be carried out in the near future.

Anti-symmetrical Curved Composite Laminate Subject to Delamination Induced by Thermal Cycling (Ref. [16])

This work was developed by Aline E. Treml (UEPG), Dr. Maurício Donadon (ITA) and co-workers.

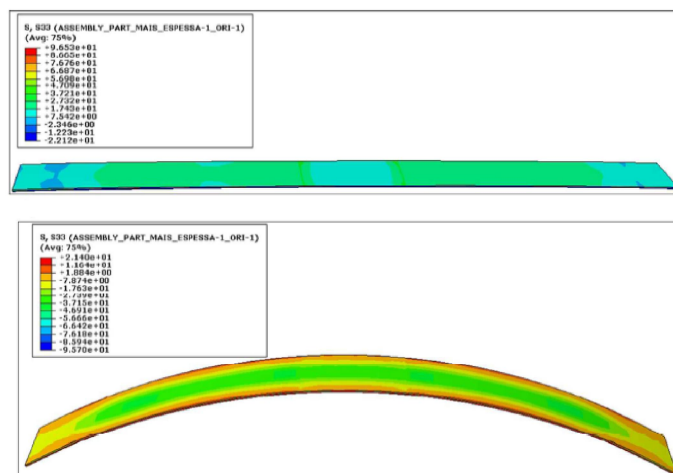
Composite structures usually undergo to temperature variations in aircraft during landing/taking off and when cruising at high altitude. Under these conditions and in combination with curved structures, they can generate severe thermal stresses that may induce delaminations.

Considering the importance of studying delamination under these conditions, this research imposed an anti-symmetrical laminate to cyclic temperature variations between -70°C and 130°C, with the objective of inducing varied curvatures and, consequently, crack growth. Different from standardized test procedures, this test set up elastically deformed coupons without external forces and numerically evaluated the Strain Energy Release Rate (SERR) during crack propagation. This procedure enabled the assessment of delamination rate (da/dN) as a function of maximum SERR.

The experimental results were compared with numerical results obtained by ABAQUS® FE code. Despite of large scatter in experimental results, a reasonable correlation between experimental and numerical results was obtained in terms of crack growth rate (da/dN) as a function of the maximum SERR.



(a)



(b)

Figure 20 – (a) Overview of the test specimens (curved laminate plates), (b) ABAQUS® analysis results - undeformed and deformed shape with 30mm crack.

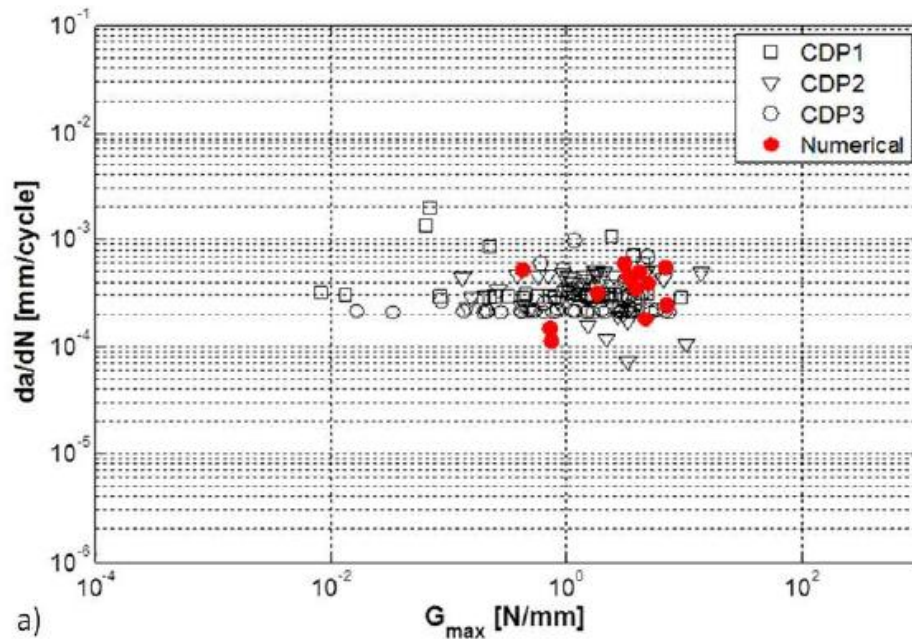


Figure 21 – Comparison of numerical and experimental Energy Release Rate.

Some selected information from the paper is included in this report. Figure 20 shows an overview of the laminate test specimens used to thermal cycling and one example of the analysis that was performed, with the undeformed and deformed shape for a certain crack size. Figure 21 shows the Energy Release Rate for both numerical and experimental results, obtained from three test specimens.

Bird Strike Modeling in Fiber-Reinforced Polymer Composites (Ref. [17])

This research work was performed by Dr. Maurício Donadon and Dr. Mariano A. Arbelo (ITA).

The related paper describes a numerical modeling approach to predict impact resistance and residual Shear Strength After Impact (SSAI) of fiber reinforced polymer composites subjected to bird strike loading. An improved damage mechanics based material model, previously developed by the authors, is combined with an equation of state to simulate the progressive failure in composite aerostructures subjected to bird strike loading. A series of bird strike impacts on flat panels fabricated from low cost woven glass composite materials are used to validate the material model for practical composite component applications. A numerical study on the residual SSAI of a typical composite shear web is also presented. The panels are modelled with shell elements only. The proposed material model formulation accounts for the strain rate enhancement to strength and shear nonlinearities observed in composite materials. A hydrodynamic model for the bird, based on 90% water and 10% air, is derived to represent the behavior of the bird for all impact scenarios considered. The bird is heterogeneous in nature.

However, a uniform material behavior is assumed with a geometry based on a 2:1 length to diameter ratio with a cylindrical body and spherical end caps using a Lagrangian mesh. Appropriate contact definitions are used between the bird and the composite panel. The simulation results were compared to experimental results and several conclusions were drawn.

Some selected results are presented in this review. Figure 22 shows, for the composite panel under analysis, the various failure modes predicted after the impact.

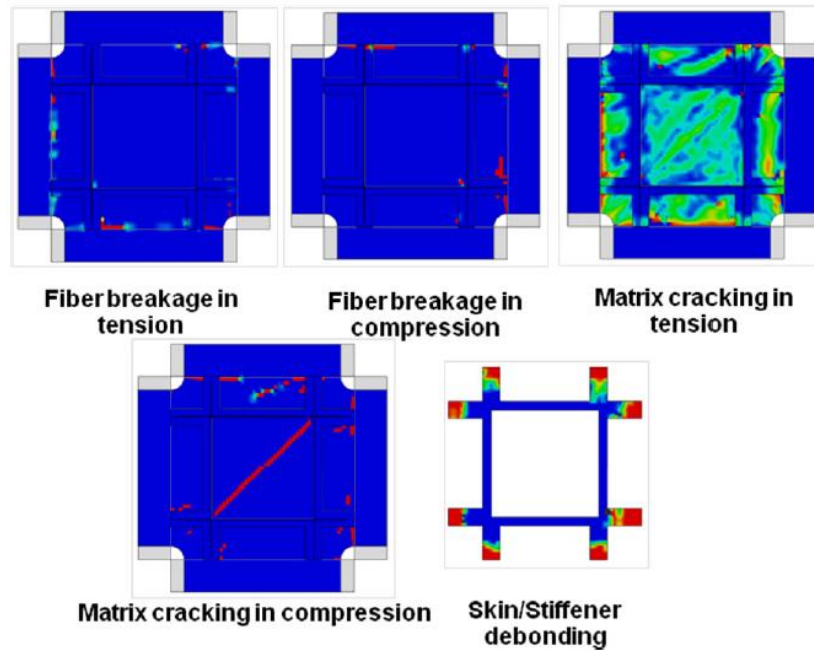


Figure 22 – Predicted failure modes for stiffened composite panel.

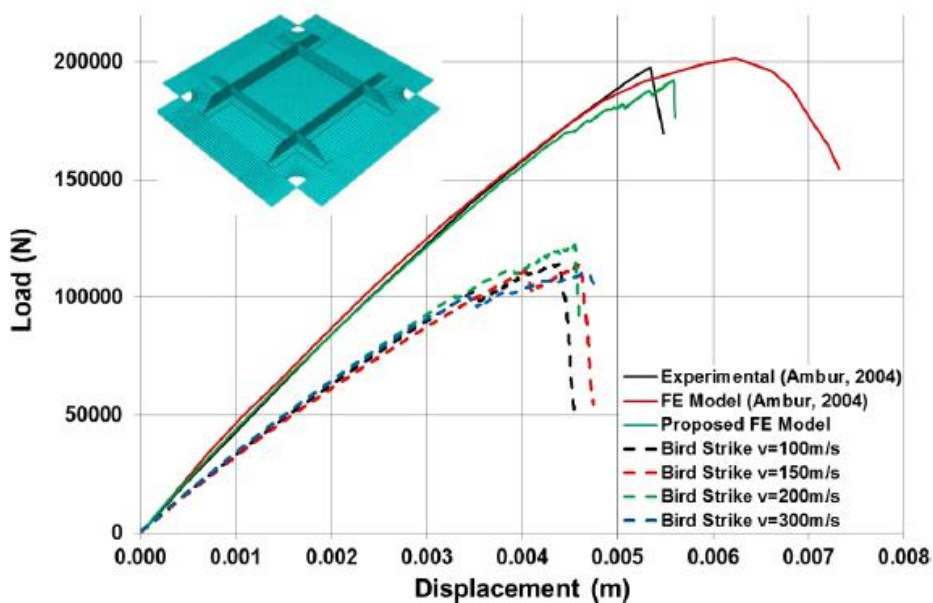


Figure 23 – Load-displacement curve for panel impacted at different velocities.

The paper described the hydrodynamic model developed for the bird, the composite failure model, a failure criteria and damage evolution laws, a rate dependent constitutive model used to model the in-plane shear behavior and a stress degradation procedure. As part of the results, Figure 23 shows the comparison of experimental results with the proposed failure model, as well as the load-displacement curve for the panel impacted at bird velocities varying from 100 m/s to 300 m/s.

Fatigue under Shear Stress by Using the Iosipescu Method for Carbon/Epoxy Composites (Ref. [18])

This work was developed by Vanderlei O. Gonçalves (DCTA) and co-workers. The work presents results on fatigue under shear stress by using the Iosipescu method (ASTM D 5379M standard). For fatigue testing a cured neat epoxy resin and a carbon fiber/epoxy composite having orientations of $0/90^\circ$ and $\pm 45^\circ$ in relation to the loading axis were tested by using the Iosipescu coupon. Firstly, the specimens were submitted to static tests in order to obtain the ultimate shear strength (τ) and the inplane shear modulus (G_{12}). Further batches of specimens were tested under pre-defined levels of stress ratio as a function of number of cycles. So, the S-N curves were obtained. The maximum number of cycles was set at 120,000 cycles, which corresponds approximately to two times the life of a structural element from a commercial airplane. The stress ratios used were set to $R=0.1$ and $R=0.5$. At the limit of 120,000 cycles the epoxy resin exhibited a shear strength of 18 MPa, for a stress ratio of $R=0.5$, and 10 MPa for a stress ratio of $R=0.1$. The carbon fiber/epoxy $0/90^\circ$ composite, at the limit of 120,000 cycles, showed a shear strength of 84 MPa for a stress ratio of $R=0.5$, and 64 MPa for a stress ratio of $R=0.1$. For the carbon fiber/epoxy $\pm 45^\circ$ composite, at the limit of 120,000 cycles, a shear strength of 105 MPa and 90 MPa, where found for a stress ratio of $R=0.5$ and $R=0.1$, respectively. The setup that was developed for these experiments is presented below in Figure 24.

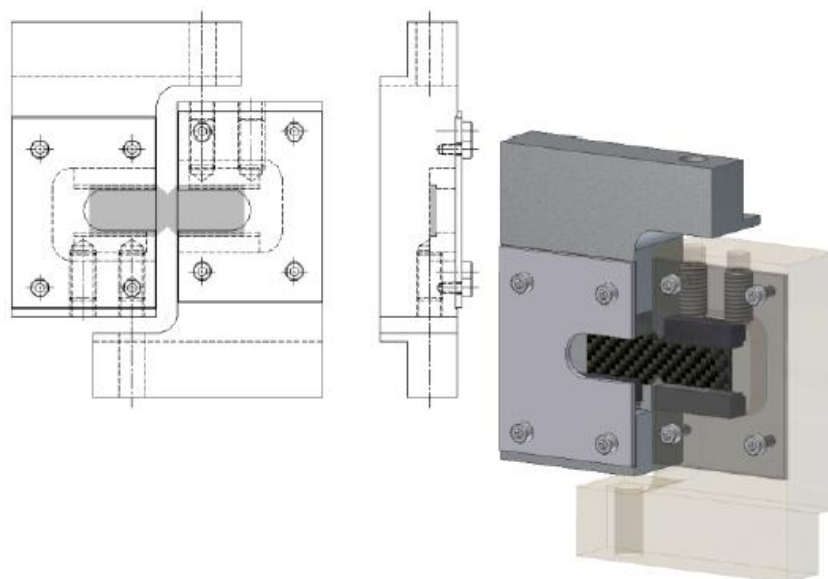


Figure 24 - Jig developed for the fatigue tests based on Iosipescu method.

The S-N curves were obtained for the neat epoxy resin, carbon fiber/epoxy 0/90° and carbon fiber/epoxy ± 45°. Figure 25 below shows the curves obtained for the neat epoxy resin.

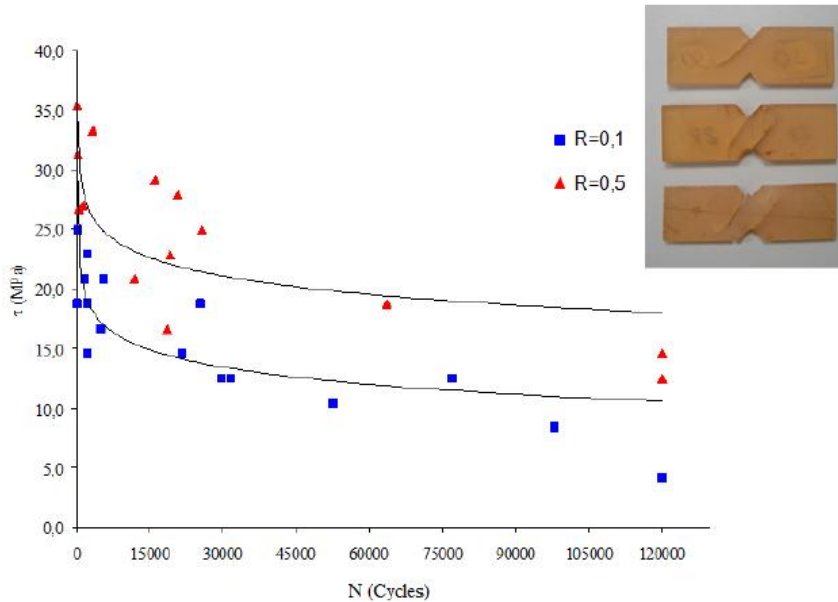


Figure 25 -S-N curves for the neat epoxy resin.

7. COMPOSITE MATERIALS – STRUCTURES

A Finite Element Modeling Strategy for Simulation of Residual Strength of Composite Panels After Impact

This topic refers to a cooperation work between Embraer R&D Department and the University of Girona (Spain).

In the event of an impact, composite structure residual strength degrades due to a large variety of failure mechanisms (matrix cracking, fiber–matrix interface debonding, delamination, and fiber breakage), which interact in a complex way. Moreover, the onset and the evolution of these failure mechanisms depend on a large set of impact parameters, which are the physical parameters and properties of the impactor, structural configuration and boundary conditions, and environmental conditions. Due to all these facts, the development of a reliable tool for the prediction of the impact damage resistance and the corresponding damage tolerance is a challenging task.

The work describes the modeling strategy for the simulation of stiffened structures under Low Velocity Impact (LVI) and Compression After Impact (CAI). Accordingly, the issues listed below were described in detail:

- FE modeling strategy
- Constitutive models related

- Key FE definitions
- Numerical predictions and comparison with experimental data of LVI and CAI tests

The simulations were performed in an explicit finite element code, using the commercial FE code Abaqus/Explicit®. All the user-defined constitutive material subroutines used were implemented in FORTRAN programming language.

After performing LVI and CAI simulations, a good correlation was observed between experimental results and FE analysis of the monolithic flat plates impacted.

Long simulation times were observed in the analyses. This is due to the complex damage models used and the need for very small element sizes.

Due to the importance of the subject in composite design of aeronautical structures, the investigation on LVI and CAI shall be continued, in order to get a better comprehension of the phenomenon regarding mechanical and especially virtual testing.

Wing Demonstrator

In Section 5 of this report, a metallic wing demonstrator incorporating innovative technologies for metallic materials and FML was presented. Besides the metallic wing demonstrator, Embraer R&D Department worked on the development and testing of a composite wing demonstrator.

The demonstrator is part of a building block encompassing a series of tests for verification of various important aspects of composite material technology, such as manufacturing integration, fatigue, flammability, lightning protection, drilling and fastening, assembly of joints, among others.

The tests were performed in ISQ (Instituto de Soldadura e Qualidade) facilities, in Portugal. Figure 26 shows an overview of the composite wing demonstrator.

8. HYBRID STRUCTURES

The addition of a section dedicated to hybrid (i.e., metallic and composite) structures is being introduced in the ICAF Brazilian National Review. This is because it has been observed an increasing usage of hybrid structures in aerospace applications, probably due to the need of pursuing the best material, either metallic or composite, for each specific application, often resulting in composite to metallic materials interfacing in regions encompassing the primary structure of the aircraft, or even interior structures subjected to high load factor requirements (like monuments).

During the last years, there are some brazilian researchers working in cooperation with two german institutions, HZG and TUHH, with novel technologies for joining hybrid structures. An overview of their research work will be presented along the following lines.

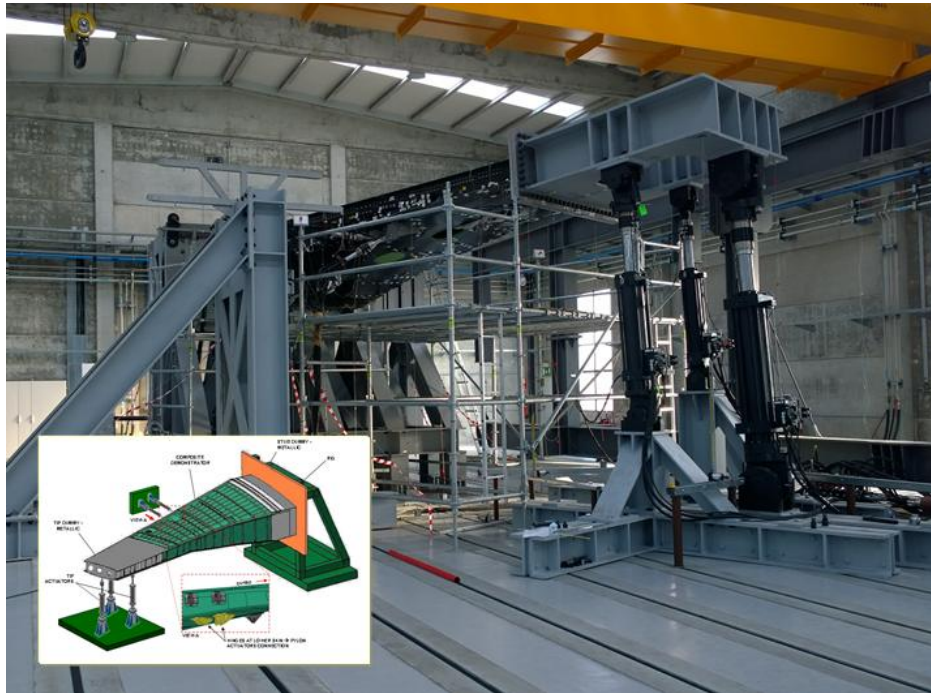


Figure 26 – Embraer composite wing demonstrator – overview.

Ultrasonic Joining: A Novel Direct-assembly Technique for Metal-composite Hybrid Structures (Ref. [20])

Ultrasonic joining (U-Joining) is a new direct assembly technique developed by HZG that uses ultra sonic energy to join fiber-reinforced thermoplastics to surface-structured metallic parts produced by metal injection molding. Ultrasonic vibration and pressure create frictional heat at the materials interface, which softens the composite matrix and allows the reinforcement (structured on the surface of the metallic part) to penetrate the composite. As a result, a metal-composite hybrid joint with improved out-of-plane strength is achieved. In this work, the features of U-Joining are briefly introduced, and the feasibility of the technique is demonstrated with Ti-6Al-4V/glass-fiber-reinforced polyetherimide joints. Optical microscopy reveals that a close contact between metal and composite was achieved after U-joining. Lap shear testing of six-pinjoints showed an improvement in strength of up to 5.5 times (2011 ± 530 N) that of pin-less reference joints (368 ± 29 N).

Figure 27 shows the specimen geometry and assessment of global mechanical performance of the joints. Additionally, force-displacement curves clearly demonstrate that the through-the-thickness reinforcement increases the quasi-static strength and ductility of the joints in comparison to the non-reinforced reference joints.

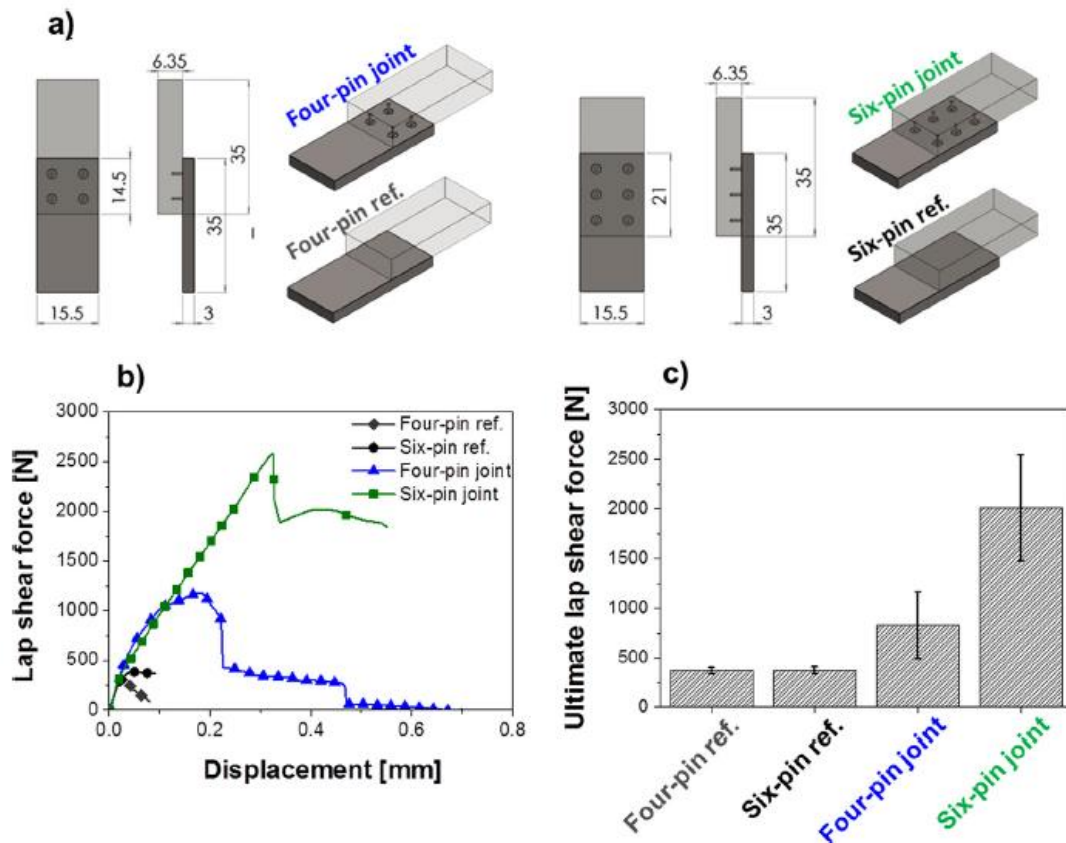


Figure 27 – (a) geometry of the lap-shear specimens (b) force -displacement curves for the best results for pin-less reference, four-and six-pin joints (c) and, average shear force for each type of joint.

Friction Spot Joining of Aluminum Alloy 2024-T3 and Carbon-fiber-reinforced Poly (Phenylene Sulfide) Laminate with Additional PPS Film Interlayer: Microstructure, Mechanical Strength and Failure Mechanisms (Ref. [21])

This research work was done in cooperation among the Federal University of São Carlos (UFSCar), HZG and TPHH.

Friction Spot Joining (FSpJ) is an innovative friction-based joining technique for metalepolymer hybrid structures. In this work, aluminum alloy 2024-T3 and CF-PPS friction-spot joints were produced with additional PPS film interlayer. The joints were investigated in terms of the microstructure, mechanical performance under quasi-static loading and failure mechanisms. Macro-mechanical and micro-mechanical interlocking as well as adhesion forces were identified to dictate bonding mechanisms in the FSp joint with film interlayer. The ultimate lap shear force of the joints (2700 ± 115 N up to 3070 ± 165 N) were 20% - 55% higher than the corresponding joints without interlayer, due to the larger bonding area, better load distribution and improved micro-mechanical interlocking. The failure analysis of the joints revealed a mixture of adhesive-cohesive failure, whereas cohesive failure was dominant.

Figure 28 shows a schematic description of the FSpJ process without the addition of film interlayer. Figure 29 shows the overview of the specimens.

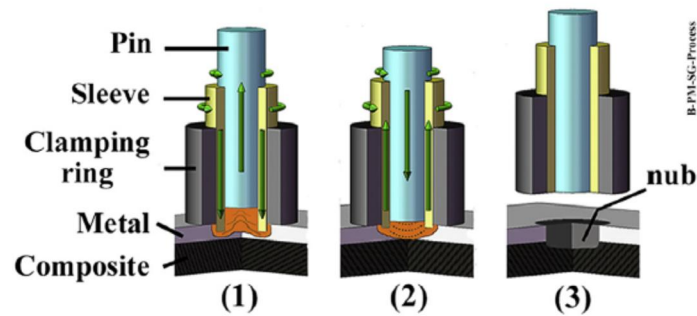


Figure 28 - FSpJ process without the addition of film interlayer. (1) sleeve plunging and plasticizing of the metal; (2) spot refilling and (3) joint consolidation.

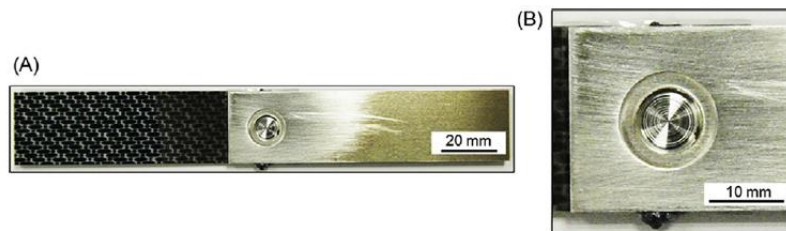


Figure 29 – (A) Top view and (B) detailed view showing the spot area of a single lap Al 2024-T3/CF-PPS FSp joint with PPS interlayer.

On the Process-Related Rivet Microstructural Evolution, Material Flow and Mechanical Properties of Ti-6Al-4V/GFRP Friction-Riveted Joints (Ref. [22])

This research work was done in cooperation among the UFSCar, HZG and TPHH.

In the work, process-related thermo-mechanical changes in the rivet microstructure, joint local and global mechanical properties, and their correlation with the rivet plastic deformation regime were investigated for Ti-6Al-4V (rivet) and glass-fiber-reinforced polyester (GF-P) friction-riveted joints of a single polymeric base plate. Joints displaying similar quasi-static mechanical performance to conventional bolted joints were selected for detailed characterization.

The mechanical performance was assessed on lap shear specimens, whereby the friction-riveted joints were connected with AA2198 gussets. Two levels of energy input were used, resulting in process temperatures varying from 460 ± 130 °C to 758 ± 56 °C and fast cooling rates (178 ± 15 °C/s, 59 ± 15 °C/s). A complex final microstructure was identified in the rivet. Whereas equiaxial α -grains with β -phase precipitated in their grain boundaries were identified in the rivet heat-affected zone, refined α' martensite, Widmanstätten structures and β -fleck domains were present in the plastically deformed rivet volume. The transition from equiaxed to acicular structures resulted in an increase of up to 24% in microhardness in comparison to the base material. A study on the rivet material flow through microtexture of the α -Ti phase and β -fleck orientation revealed a

strong effect of shear stress and forging which induced simple shear deformation. By combining advanced microstructural analysis techniques with local mechanical testing and temperature measurement, the nature of the complex rivet plastic deformational regime could be determined.

9. STRUCTURAL HEALTH MONITORING

Five works (four from the Academy and one from the Industry) related to inspections and Structural Health Monitoring (SHM) will be discussed along this report.

Recent Developments in Structural Health Monitoring in the GRAVI Group in UFMG (Ref. [23])

Simple Attempt to Compensate Temperature Variation in Structural Health Monitoring Systems Using Lamb Wave Inspection (Ref. [24])

These two papers, from the same authors, are related each other and will be briefly described in this section.

The papers summarize the recent experience of the GRAVI Group¹ in SHM, due to a partnership with Embraer. The first paper describes the use by this group of Lamb Waves to detect damage in structures and the development of a software named “LaWadeUFMG” (Lamb Wave Detection), the software was developed in Matlab to control the generation, acquisition, storing, and processing of Lamb Waves using a PXI modular hardware composed by an arbitrary wave generator up to 100 MHz, two acquisition board with 8 channel each up to 60 MHz and a relay commutation matrix with 31 channels. The methods and devices developed for LW inspections were validated by means of composite and aluminium panels, as shown in Figure 30.

In the second paper, a discussion about temperature considerations in LW is presented. The temperature variation can lead to false positives due to differences in between the baseline data and the verification data. In order to avoid false positives, the work shows a simple technique to correct the experimental data to eliminate the false positives that arise due to temperature variations, by modifying their threshold values. The proposed technique was tested in the square composite plate using LW inspection based in two inspection methods. The first method is based on the construction of the wave propagation map calculated using the group velocity of the wave propagation and the Hilbert Transform. The second method is based on the comparison of the Power Spectrum Density of the signal measured by the sensors.

¹ Grupo de Acústica e Vibração.

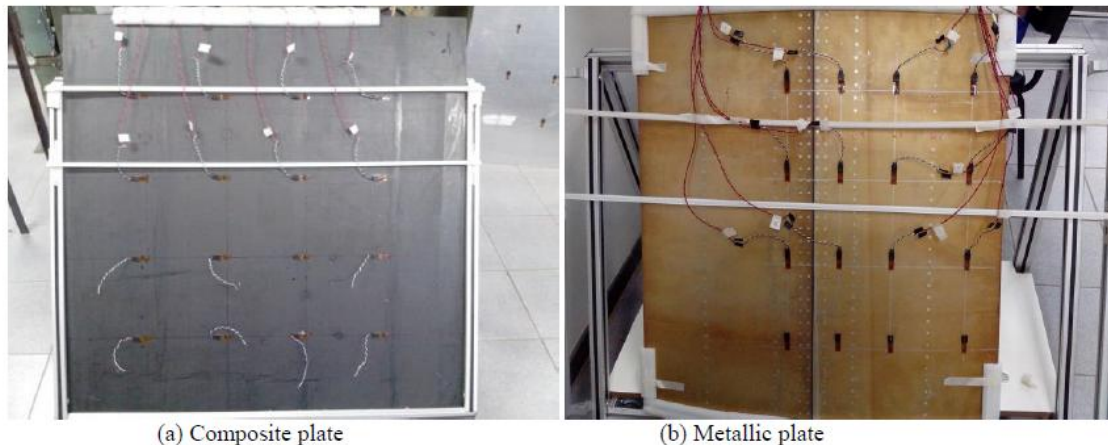


Figure 30 – (a) Composite and (b) metallic panels used for validation of LW experiments.

Damage Detection in Composite Materials Via Optimization Techniques Based on Dynamic Parameters Changes (Ref. [25])

Crack Detection in Composite Laminated Plates Using Optimization Techniques Based in Changes in Natural Frequencies (Ref. [26])

These two papers, from the same authors, are related each other and will be briefly described in this section.

In the first work, the authors employed the Finite Element Method due to the complexity of an anisotropic material (carbon fiber composite) with several layers of laminated material, which does not adapt using the contour methods that are widely used for structures with two-dimensional simplification. Optimization using heuristic methods such as genetic algorithm (GA) were used as the optimization procedure enabling to find a global optimum efficiently, allowing to properly locate the damage, avoiding the need for derivatives valuation the objective function, which could become a problem for cases where discontinuities may be present. The optimization routines of damage detection were performed using the MATLAB® software working linked with the commercial finite element software ANSYS® for creation of direct and inverse problems. Numerical test cases were employed to evaluate the performance of the algorithms in predicting the damaged parameters and pros and cons of each algorithm were summarized.

The following conclusions were drawn from this first work: (a) natural frequencies proved to be a good criterion for detecting the existence of an arbitrary structural damage. However, there are limitations on the quantification of the damage (location and size); (b) Pareto front optimization found to be the best method for detection of multiple damage, because it offers a set of feasible optimal solutions to solve the problem inserted, being one of our choice smaller distance relative to the origin (zero). The multi-objective optimization criterion for forming the front of Pareto took into account controlled elitism, which was superior to the goals of weighting technique and

difficulties appear normal at the time of insertion measurement noise in damage detection process.

In the second work, the authors modelled a structure by means of a FEM method and employed heuristic techniques coupled to this model, such as genetic algorithms, to minimize objective functions, written in terms of the dynamic parameters of the analyzed structure (natural frequencies). The structure studied is constituted of a damaged laminate of carbon fiber with a crack model induced on it. The result of the optimization algorithms showed good efficacy in the detection of structural damage.

Developments Towards the Qualification of Two SHM Systems for S-SHM Application (Ref. [27])

General: in order to understand the various aspects of Structural Health Monitoring (SHM), over the years Embraer R&D Department has investigated many different SHM technologies. Less complex and less time-consuming procedures – when compared to current NDT technologies – allowed by SHM can not only reduce the amount of time and burden of the inspection tasks, but also minimize the effects of “human-factors” when compared to current inspection procedures.

Tests were performed in an E-Jets flight tests aircraft with two different SHM technologies which were considered as promising ones for monitoring structural components. Sensors, cables and connectors of Comparative Vacuum Monitoring (CVM™) and Lamb Waves (LW) were installed as part of the developments for the qualification of the two systems. Aircraft scheduled maintenance can take advantage of these systems. Scheduled Structural Health Monitoring (S-SHM) application type considers the installation of sensors and cables into the aircraft for periodic scheduled structural inspections, these inspections being performed on-ground with ground support equipment.

Besides the installations in an E-Jets flight tests aircraft, Embraer developed Service Bulletins for the installation of the S-SHM systems in different areas of an airline’s E-Jets aircraft. Figure 31 shows as examples some sensors and cables installed in an operator’s aircraft. Over a fixed period of time, Embraer intends to collect data from the installed S-SHM systems at least four times, aiming to identify if they are operating properly in a normal operating environment. For this qualification program, laboratory tests will also be performed with CVM and LW using structural samples that represent the monitored areas of an aircraft. These lab tests will provide data for generating Probability of Detection (POD) curves for both CVM and LW systems. Embraer representatives will participate in all tests conducted. All the information will be compiled and analyzed by Embraer teams and a data package will be created to provide support for the verification of the SHM solutions as a first step in this qualification effort.

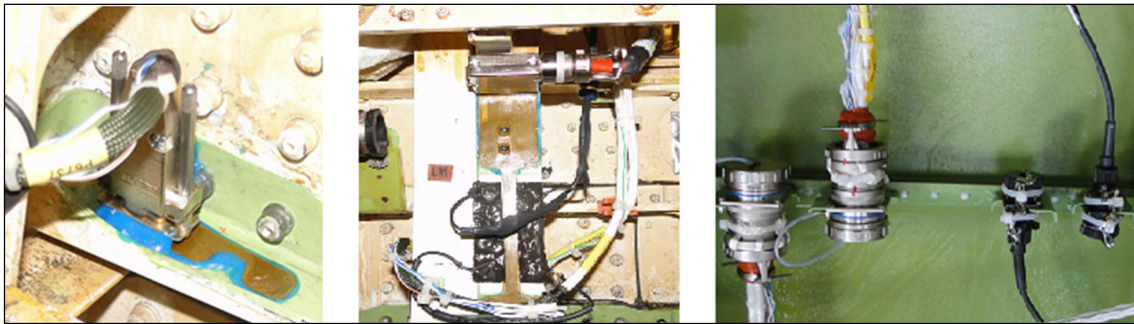


Figure 31 - Sensors and cables installed in an operator's aircraft.

SHM Damage Detection Technologies Application Types: according to the definitions from the Airlines for America (A4A) MSG-3 document and to the ARP-6461 document from SAE International, there are two distinct types of application for SHM technologies: S-SHM for Scheduled Structural Health Monitoring which means the use of SHM devices for inspections at an interval set at a fixed schedule; and, A-SHM for Automated Structural Health Monitoring that relies on the SHM system to inform maintenance personnel that action must take place.

In the Embraer perspective, S-SHM application type considers the installation of SHM sensors, cables and connectors into the aircraft with periodic scheduled structural inspections being performed on-ground with ground support equipment. And, the A-SHM application type will be the installation of not only sensors, cables and connectors, but also SHM interrogators and data recorders into the aircraft. In such a case, the structural inspections would be performed automatically at any time in smaller time intervals (or continuously), what would require to the system to have a power supply during the regular aircraft operation.

These two types of SHM application have different requirements depending on the presence of components, such as interrogators, installed in the aircraft, eventually powered up during flight.

In order to improve the conditions for SHM to be an effective part of current and future commercial aviation maintenance programs, these points must be properly addressed and Embraer is committed to it.

Due to the relevance of the structural inspections for the continuous airworthiness of any aircraft, the road to the qualification of SHM systems is not an easy task and requires the involvement of several Embraer teams.

S-SHM Qualification Effort: as part of the damage detection systems' qualification effort, a program for generating laboratory test data and systems' operational test data is under way.

Laboratory test data will cover Probability of Detection (POD) and some Environmental Tests with specimen configurations prepared for both Comparative Vacuum Monitoring and Lamb Waves.

The POD method can be used to compare the probability of detection between distinct types of inspections. Also, it provides information about the corresponding level of

confidence that can be statistically verified for each measurement. The target is to confirm that CVMTM and LW solutions have at least 90% probability of detection with 95% of confidence, for specific scenarios. The laboratory tests will use structural specimens that are representative of regions from an Embraer aircraft structure.

An approach for POD determination is the method described in the document MIL-HDBK-1823A, which was originally created for traditional NDT equipment. Another approach for assessing the system's detection capability in terms of POD is the One-Sided Tolerance Interval methodology (Ref. [28]). Apparently, both methods are suitable for SHM; however, further discussions are still required.

10. FATIGUE LIFE MONITORING

One paper about fatigue life monitoring was selected for this report. This work was developed by Danilo C. Branco (FAB) and Dr. Flavio L. S. Bussamra (ITA). The paper contents are summarized along the following lines.

Fatigue Life Monitoring System for Aircraft to Flexibilize Operations and Maintenance Planning (Ref. [29])

The damage tolerance analysis, which uses the force structural management plan, is usually employed in airplane fatigue life prediction. This plan, based on a mission "mix" defined at the airplane structure design phase, induces the squadrons to follow this mix and interferes in the fleet's usage efficiency. Deviations in the mission mix have impacts on inspection intervals and maintenance costs.

In this paper, a fatigue life monitoring system is proposed. It is able to incorporate each mission, individually, in a specific aircraft's fatigue life analysis, adjusting the maintenance plan into a more realistic usage profile, based on the individual aircraft tracking methodology. This monitoring system is implemented in a computer software and it is applied to F-5E fighter aircraft of the Brazilian Air Force. In addition, experimental fatigue tests that simulate critical locations of this aircraft were compared with the proposed monitoring system, which shows ability to predict, in conservative and approximate ways, the crack length after each flight, disregarding the predefined mission mix. This makes the flexibilization of the operations possible without jeopardizing the inspection and maintenance planning.

Some selected methods and results from the paper are presented in this review. Figure 32 shows the test setup, where simple compact specimens (whose dimensions are shown in Figure 33) were submitted to complex loading.

Figure 34 shows the results from the software developed by the author with previous DTA (made by SwRI) predictions and the actual experimental crack growth data. Additional comparison results are presented in the paper.



Figure 32 – Test Setup

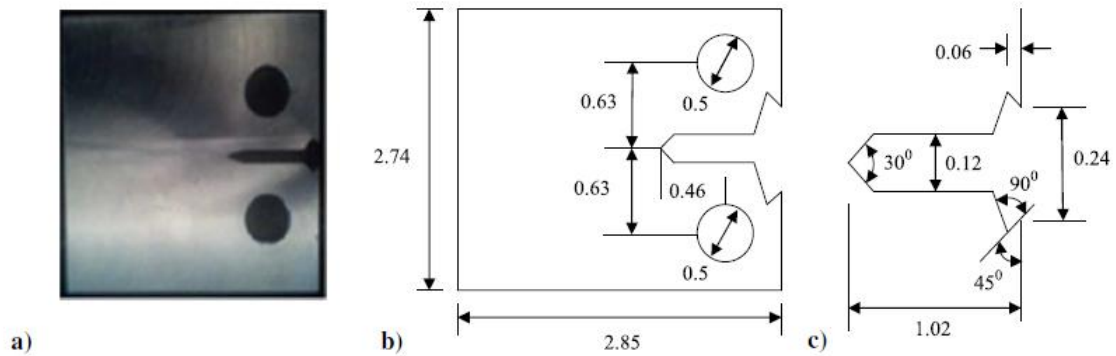


Figure 33 - Aluminum 7049-T73 compact test sample (dimensions in inches):
a) photography of test sample, b) sizes of test sample, and c) zoom of notch area

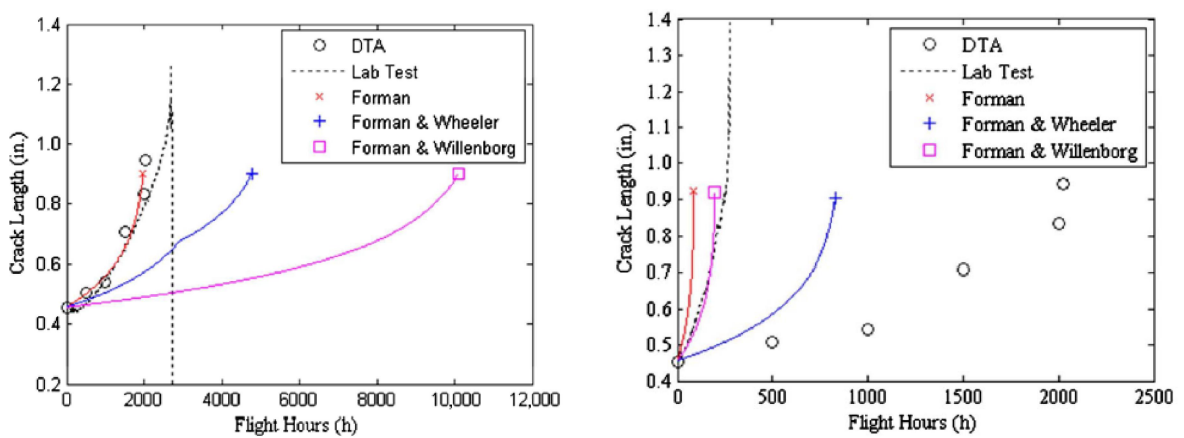


Figure 34 – Comparison between developed software (applying the Forman Theory in this case), DTA and test for (a) an average severity usage (b) a high severity usage.

11. MISCELLANEOUS

The LISA Project

The LISA (Lightweight Integral Structures for Future Generation Aircrafts) Project is a cooperation work that is being carried out during the last years with Embraer R&D Department and HZG. The main focus of this project is the investigation of FSW, laser modification and friction surfacing, with the purpose to improve the damage tolerance behavior of stiffened aluminium structures.

The LISA project is underway, many results have already been published by HZG and future works resulting from this project are expected for the next years.

The PROF Project (Ref. [30])

The PROF (Prediction of Fatigue in Engineering Alloys) Project is being coordinated by NLR, with industrial partners, including Embraer R&D Department. This project aims to increase the understanding on the physics of fatigue crack growth.

The project duration is four years and the research will be performed at the NLR. There will be various working packages to evaluate several aspects of crack growth behavior, such as the influence of (a) stress range R , (b) thickness, (c) environment, (d) crack nucleation and short crack growth behavior, (e) variable amplitude loading. Embraer will supply some materials for the specimens and participate of many phases of the project development.

More information about this project will be presented in the National Review of the Netherlands.

MACMS 2015

In December of 2015, in the University of São Paulo, Campus of São Carlos, it was held the MACMS 2015 - Meeting on Aeronautical Composite Materials and Structures. Despite of being a meeting with a wider scope including design, engineering and manufacturing technologies related to composite materials, many papers presented during that event were related to fatigue, damage tolerance, structural health monitoring and structural integrity of structures with composite materials, including works from brazilian researchers and works developed by researchers from foreign institutions.

The proceedings from MACMS 2015 were made available for downloading from the University of São Paulo website in March 2017. The related link is shown in Ref. [31].

12. REFERENCES

1. Chaves, C. E., *A Review of Aeronautical Fatigue Investigations in Brazil*, International Committee on Aeronautical Fatigue (ICAF), Helsinki – Finland – June, 2015.
2. Stoianov Cotta, I. F., *Splitting Method in Multisite Damage Solids: Mixed Mode Fracturing and Fatigue Problems*, PhD Thesis, University of São Paulo, 2015.
3. Stoianov Cotta, I. F., Proença, S. P. B., *The Splitting Method and the Generalized Finite Element Method in the Two-dimensional Analysis of Linear Elastic Domains with Multiple Cracks*, Latin American Journal of Solids and Structures, Vol. 13, pp. 2573-2605, 2016.
4. Argôlo, H. S., Proença, S. P. B., *Splitting Method and Hybrid-Trefftz Formulation for Multisite Damage Analysis in Two-dimensional Domains*, International Journal of Solids and Structures, Vol. 104-105, pp. 50-64, 2017.
5. Pascoal Jr, F. A., Aleixo, G. T., Chaves, C. E. Bose Filho, W. W., *Microstructural Analysis, Fracture Toughness and Fatigue Life of AA7050-T7451 and AA2050-T84 Alloys*, ICAF 2017, Nagoya, Japan, June 7-9, 2017.
6. Carvalho, A. L. M., Martins, J. P., *Effect of Interrupted Ageing and Retrogression-Reageing Treatments on Fatigue Crack Growth with a Single Applied Overload in 7050 Aluminum Alloy*. Metallurgical and Material Transactions, submitted for publication.
7. Carvalho, S. M., Lima, M. S. F., Baptista, C. A. R. P. 2, Siqueira, A. F., *Fatigue in Laser Welded Titanium Tubes Intended for Use in Aircraft Pneumatic Systems*, International Journal of Fatigue, Vol. 90, pp. 47–56, 2016.
8. Cunha, M. C., Lima, M. S. F., *The Influence of Laser Surface Treatment on the Fatigue Crack Growth of Aluminum Alloy Sheet*,
9. Almeida, R. Z. H., Carunchio, A. F., Mendonça, W. R. P., *Comparison Between Fatigue Performance of Two Different Aircraft Riveted Joints*, presented in the 23rd ABCM International Congress of Mechanical Engineering, December 6-11, 2015, Rio de Janeiro, RJ, Brazil.
10. Spangel, S., Miermeister, M., Gijbels, J., Fernandez, F. F., Nunes, D. F. S., Miyazaki, M., *Manufacturing of an Advanced Wing Spar by FSW*, 24th ASM Aeromat Conference, Orlando – FL, USA, June 16-19, 2014.
11. Nunes, D. F. S., Cruz, M., Mendonça, W. R. P., Brandão, F. M., Sakata, A., Silva, G., Kulak, M., *Manufacturing of a Fiber Metal Laminate Lower Wing Cover Demonstrator*, 28th ASM Aeromat Conference, Charleston – SC, April 10-12, 2017.
12. Shiino, M. Y., Alderliesten, R. C., Donadon, M.V., Cioffi, M.O.H., *The Relationship Between Pure Delamination Modes I and II on the Crack Growth Rate Process in*

- Cracked Lap Shear Specimen (CLS) of 5 Harness Satin Composites, Composites Part A: Applied Science and Manufacturing, Composites Part A: Applied Science and Manufacturing, Vol. 78, pp. 350-357, 2015.
13. Shiino, M. Y., Alderliesten, R. C., Donadon, M. V., Voorwald, H. J. C., Cioffi, M. O. H., *Applicability of Standard Delamination Tests (Double Cantilever Beam and End Notch Flexure) for 5HS Fabric-reinforced Composites in Weft-dominated Surface*, Journal of Composite Materials, September 2014.
 14. Leite, B. M., Leite, L. F. M., Reis, V. L., Donadon, M. V., *A Numerical Study on Testing Configurations for Intralaminar Fiber Kinking Fracture Toughness Characterization of Composites in The Dynamic Regime*, BCCM-3 – Brazilian Conference on Composite Materials, Gramado, RS - Brazil, August 28-31, 2016.
 15. Leite, L. F. M., Leite, B. M., Reis, V. L., Donadon, M. V., *A Numerical Study on Testing Configurations for Intralaminar Tensile Fracture Toughness of Composites in The Dynamic Regime*, BCCM-3 – Brazilian Conference on Composite Materials, Gramado, RS - Brazil, August 28-31, 2016.
 16. Treml, A. E., Gouvêa, R., Sales, R. C. M., Donadon, M. V., Shiino, M. Y., Bressan, J. D., *Anti-symmetrical Curved Composite Laminate Subject to Delamination Induced by Thermal Cycling*, Fatigue and Fracture of Engineering Materials and Structures, 2017.
 17. Donadon, M. V., Arbelo, M. A., *Bird Strike Modeling in Fiber-Reinforced Polymer Composites*, International Journal of Structural Stability and Dynamics, Vol. 17, No. 4, 2017.
 18. Gonçalves, V. O., Pardini, L. C., Ancelotti Jr., A. C., *Fatigue under Shear Stress by Using the Iosipescu Method for Carbon/Epoxy Composites*, Advanced Engineering Forum, Vol. 20, pp. 22-28, 2016.
 19. Marques, L. C., Composite R&D Challenges for EMBRAER Aerostructures, SAMPE Summit 2017, Paris, March 03, 2017.
 20. Feistauer, E. E., Guimarães, R. P. M., Ebel, T., dos Santos, J. F., Amancio-Filho, S. T., *Ultrasonic joining: A novel Direct-assembly Technique for Metal-composite Hybrid Structures*, Materials Letters, Vol. 170, pp. 1-4, 2016.
 21. André, N. M., Goushegir, S. M., dos Santos J. F., Canto, L. B., Amancio-Filho, S. T., *Friction Spot Joining of Aluminum Alloy 2024-T3 and Carbon-fiber-reinforced Poly (Phenylene Sulfide) Laminate with Additional PPS Film Interlayer: Microstructure, Mechanical Strength and Failure Mechanisms*, Composites Part B, pp. 197-208, 2016.
 22. Borba, N. Z., Afonso, C. R. M., Blaga, L., dos Santos J. F., Canto, L. B., Amancio-Filho, S., *On the Process-Related Rivet Microstructural Evolution, Material Flow and Mechanical Properties of Ti-6Al-4V/GFRP Friction-Riveted Joints*, Materials, Vol. 10(2), pp. 184, 2017.
 23. Donadon, L. V., Ferreira, L. P. S., Duarte, H. V., *Recent Developments in Structural Health Monitoring in the GRAVI Group in UFMG*, COBEM 2015, 23rd ABCM



International Congress of Mechanical Engineering, December 6-11, 2015, Rio de Janeiro, RJ, Brazil.

24. Donadon, L. V., Ferreira, L. P. S., Duarte, H. V., Medeiros, E. B., Simple Attempt to Compensate Temperature Variation in Structural Health Monitoring Systems Using Lamb Wave Inspection COBEM 2015, 23rd ABCM International Congress of Mechanical Engineering, December 6-11, 2015, Rio de Janeiro, RJ, Brazil.
25. Gomes, G. F., Cunha Jr., S. S., Ancelotti Jr., A. C., Melo, M. L. N. M., *Damage Detection in Composite Materials Via Optimization Techniques Based on Dynamic Parameters Changes*, International Journal of Emerging Technology and Advanced Engineering, Volume 6, Issue 5, May 2016.
26. Gomes, G. F., Cunha Jr., S. S., Ancelotti Jr., *Crack Detection in Composite Laminated Plates Using Optimization Techniques Based in Changes in Natural Frequencies*, International Journal of Engineering Applied Sciences and Technology, Vol. 1, No. 1, Pages 1-6, 2015.
27. Rulli, R. P., Dotta, F., *Developments Towards the Qualification of Two SHM Systems For S-SHM Application*, 10th International Workshop on Structural Health Monitoring, IWSHM, Stanford – CA, September 1-3, 2015.
28. Roach, D. P., *Validation and Verification Processes to Certify SHM Solutions for Commercial Aircraft Applications*, 9th International Workshop on Structural Health Monitoring, Stanford – CA, September 10-12, 2013.
29. Branco, D. C., Bussamra, F. L. S., *Fatigue Life Monitoring System for Aircraft to Flexibilize Operations and Maintenance Planning*, Journal of Aircraft Vol. 53, No. 5, September-October 2016.
30. Amsterdam, E., *Prediction of Fatigue in Engineering Alloys (PROF)*, NLR Proposal, July. 2016.
31. MACMS 2015, Meeting on Aeronautical Composite Materials and Structures <http://soac.eesc.usp.br/index.php/macms/macms/schedConf/presentations>, ISBN/ISSN:978-85-8023-050-5.